



Matematica e Medicina: CELLULAR POTTS MODEL

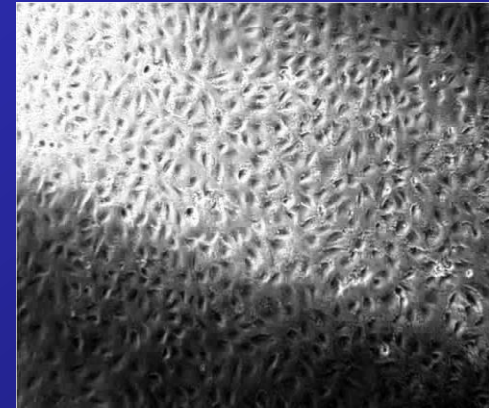
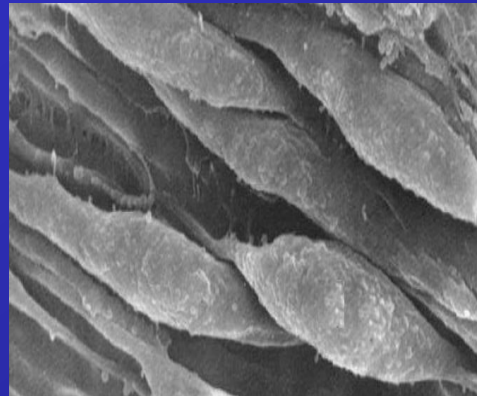
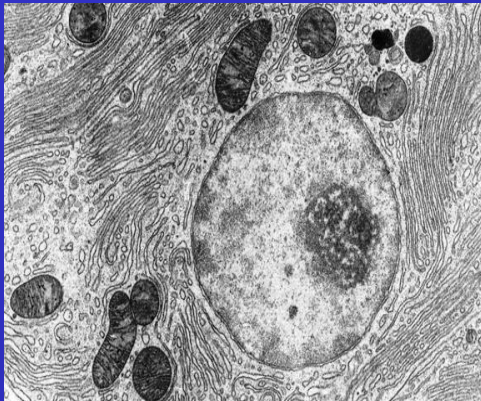
Marco SCIANNA

Politecnico di Torino

INTRODUCTION



All biological phenomena emerge from intricate interactions between multiple levels of organization:



$\ll 10^{-7}$ m

microscopic level

- ✓ protein cascades
- ✓ chemical diffusion
- ✓ gene networks

10^{-6} m

mesoscopic level

- ✓ cell division
- ✓ adhesion
- ✓ migration

$\gg 10^{-5}$ m

macroscopic level

- ✓ tissue growth
- ✓ population dynamics
- ✓ multicellular patterns

INTRODUCTION



Mathematical approaches for biological problems employ a wide range of techniques, depending on the scale of interest:

microscopic scale	mesoscopic scale	macroscopic scale
$\ll 10^{-7}$ m	10^{-6} m	$\gg 10^{-5}$ m
subcellular level	cellular level	tissue level
RD SYSTEMS	INDIVIDUAL BASED MODELS	CONTINUOUS METHODS
✓ systems of ODEs or PDEs	✓ discrete	✓ systems of PDEs
✓ kinetics equations	✓ phenomenologic	✓ populations as densities
	✓ object-oriented	✓ balance laws

However, the use of a single specific type of model may be often unsatisfactory

MATHEMATICAL MODEL



The CELLULAR POTTS MODEL is:

- ✓ a hybrid and flexible individual-based approach, focused on the phenomenology of cell-level individuals (cells, ECM fibers, unicellular organisms,...)
- ✓ formed by a list of discrete individuals with phenomenological rules for their dynamics and interactions
- ✓ a Monte Carlo iterative method, based on an energy-minimization philosophy driving how the simulated individuals behave

MATHEMATICAL MODEL



The Cellular Potts Model (CPM) is a lattice-based Monte Carlo technique which follows an iterative and stochastic energy-minimization philosophy

a CPM domain is a d -dimensional lattice (i.e., a regular grid formed by identical d -dimensional lattice sites \underline{x}), where $d=2,3$. Each site is identified by an integer number, called spin, $\sigma(\underline{x})$

a set of contiguous lattice sites labeled by

the same spin σ form a single object, a discrete physical unit Σ_σ with a relative type $\tau(\Sigma_\sigma)$

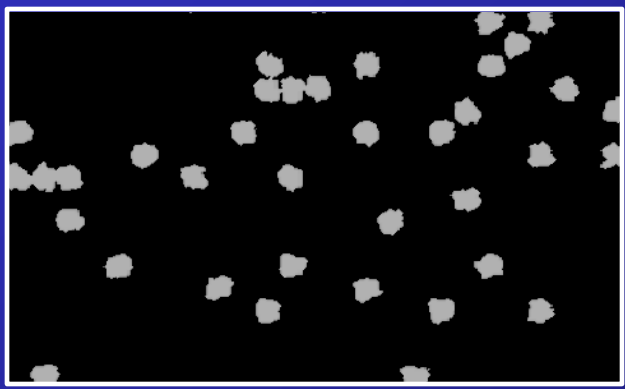
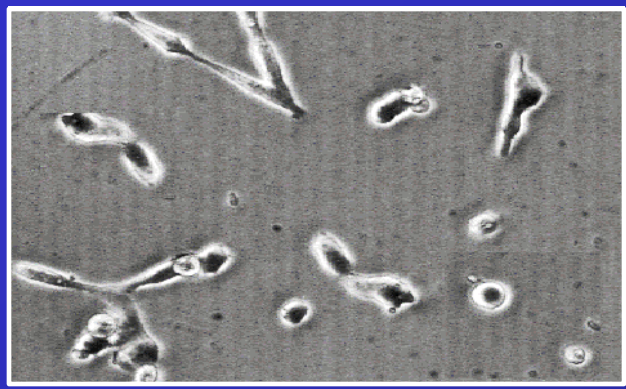
connections between neighboring lattice sites of unlike state σ represent objects' membranes

4	4	4	4	0	0	0
4	2	2	2	0	0	0
1	2	2	3	3	3	0
1	1	3	3	3	3	0
1	1	3	3	3	5	5
6	6	3	3	5	5	5
6	6	3	3	5	5	5

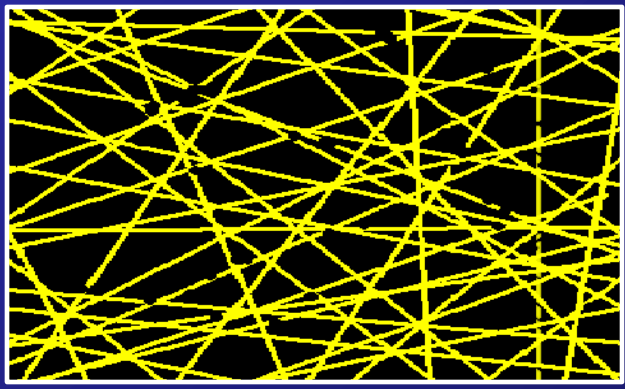
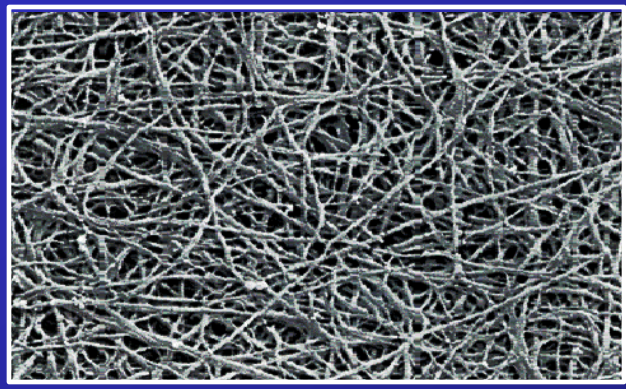


MATHEMATICAL MODEL

Grid subdomains may represent entire single biological elements



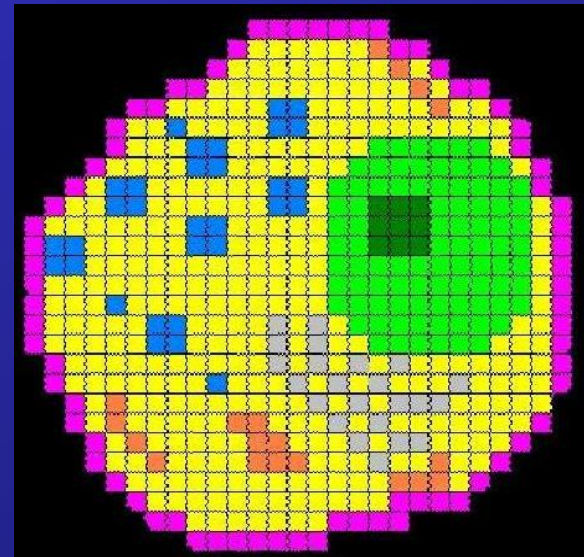
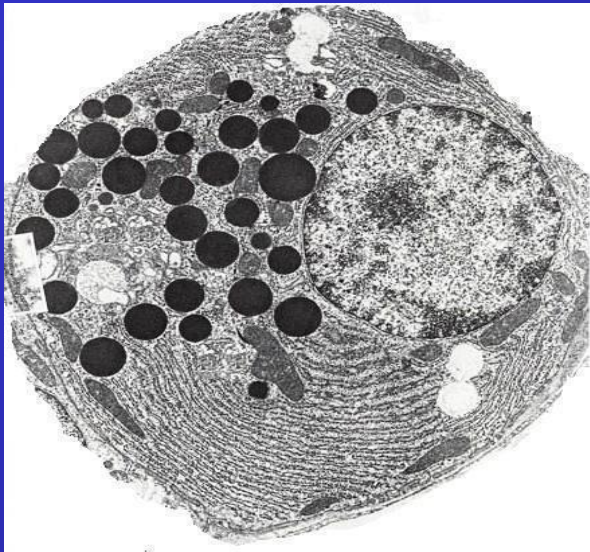
cells



matrix fibers

MATHEMATICAL MODEL

...or element subcompartments, for example their intracellular compartments (nucleus, cytosol, PM, Golgi Apparatus, ER, ...) and organelles (mitochondria, ...)



However, the more detailed is the cell representation, the more the model is computationally expensive.

MATHEMATICAL MODEL



The system energy is defined with an Hamiltonian H , which consists in the sum of terms relative to:

- ✓ adhesion between individuals (Steinberg's DAH)

$$H_{\text{adh}} = \sum_{x,x'} J_{\sigma(x),\sigma(x')} (1 - \delta_{\sigma(x),\sigma(x')})$$

- ✓ individual attributes (volume, surface, velocity,...)

$$H_{\text{attr}} = \sum_{i\text{-attribute},\sigma} [\lambda_{\sigma}^i (a_{\sigma}^i(\text{t. v.}) - A_{\sigma}^i(\text{a. v.}))^2]$$

- ✓ effective and generalized forces (potential, chemotaxis, ...)

$$H_{\text{force}} = - \sum_{k\text{-force},\sigma} [\mu_{\sigma}^k F_{\sigma}^k]$$

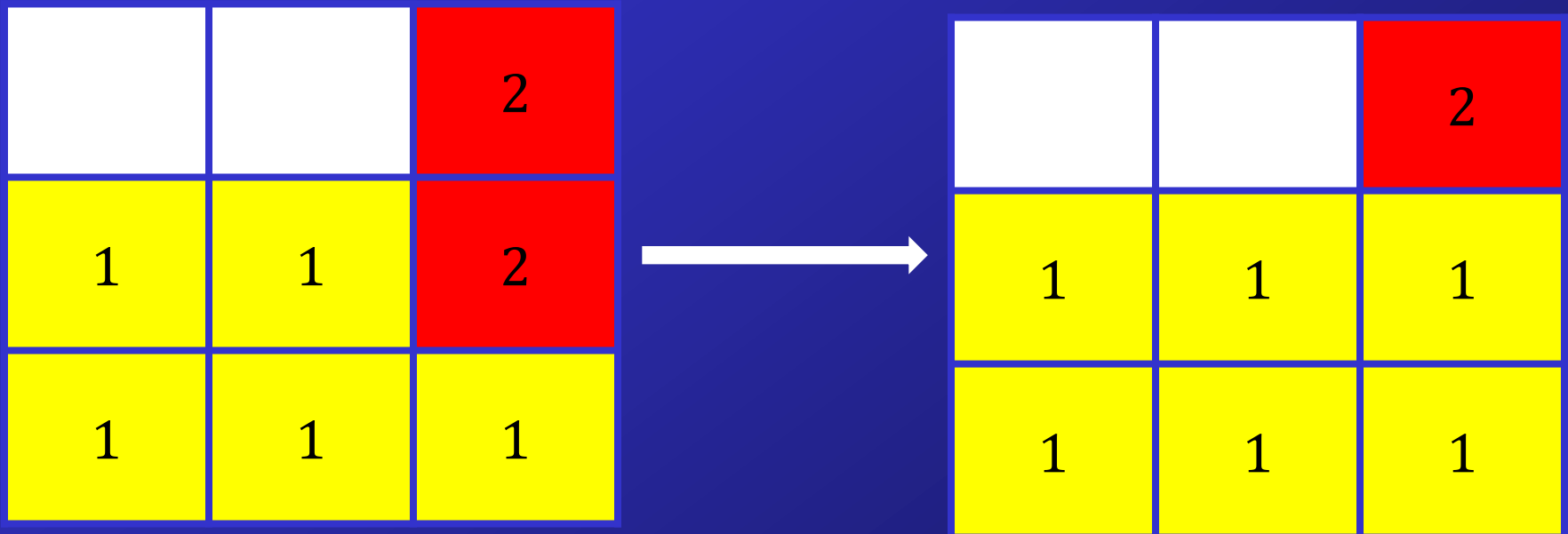
$J_{\sigma(x),\sigma(x')}$, λ_{σ} and μ_{σ} are Potts coefficients describing the importance of the relative biophysical properties or mechanisms

MATHEMATICAL MODEL



Individuals move and behave in order to iteratively and stochastically reduce H , with a simple algorithm:

- 1- choose a lattice site belonging to an individual membrane and attempt to copy its spin into a randomly chosen neighboring lattice site



- 2- the difference in the system energy as a results of the attempt is calculated:

$$\Delta H = H_{\text{after spin copy}} - H_{\text{before spin copy}}$$

MATHEMATICAL MODEL

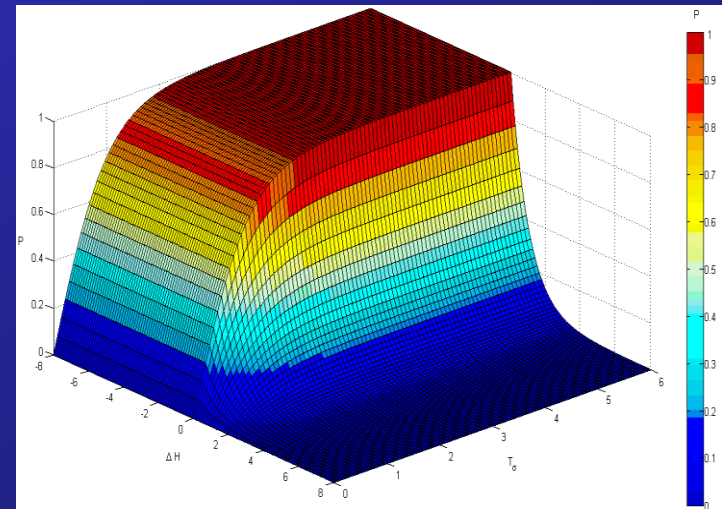
3- the attempt is accepted with a Boltzmann-like probability:

$$P(\Delta H) = p(T_{\text{moving object } \Sigma\sigma}) \min\{1, \exp(-\Delta H / T_{\text{moving object } \Sigma\sigma})\},$$

where

- ✓ $T_{\text{moving object } \Sigma\sigma}$ is the agitation rate of the object moving site belongs to
- ✓ p is a maximum transition probability function characterized by:

$$\left\{ \begin{array}{l} p(0) = 0 \\ \lim_{T \rightarrow +\infty} p(T_{\text{moving object}}(t)) = 1 \end{array} \right.$$



4- the algorithm is repeated until the system reaches a global minimum or until a given observation time. Each iteration is defined a Monte Carlo Step

MATHEMATICAL MODEL



The model can be finally integrated by the evolution of molecular variables (i.e., ions, molecules, or genes) localized both within biological elements (within one of their subcompartments) and/or in the extracellular space. The dynamics of such microscopic variables are modelled by typical and suitable reaction-diffusion equations:

$$\frac{\partial c(x)}{\partial t} = D_c \frac{\partial^2 c}{\partial x^2} - a c + s$$

variation of c within point x at time t

diffusion

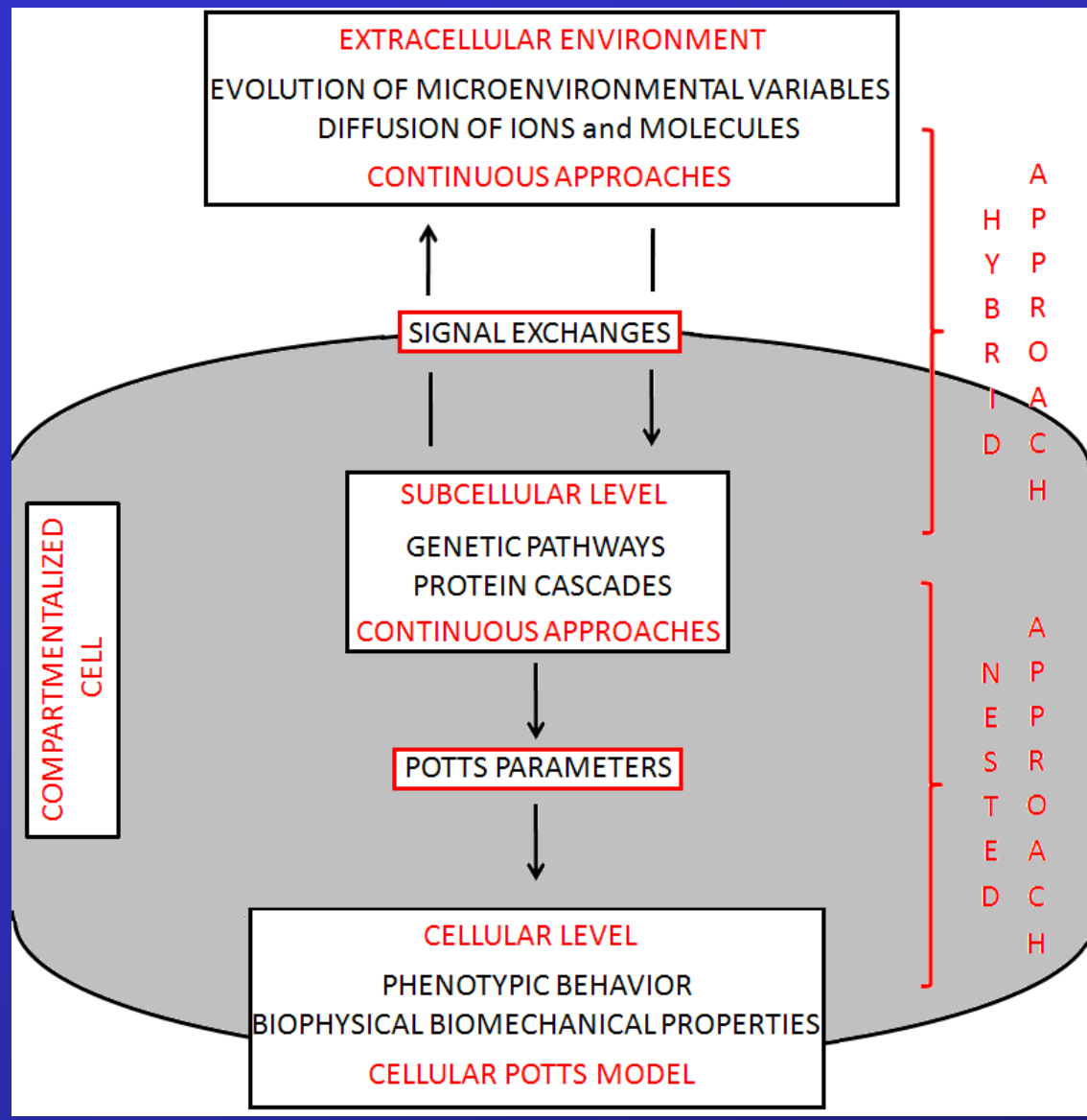
decay

production

Finally, we need to define constitutive laws describing how the molecular elements influence cell behavior



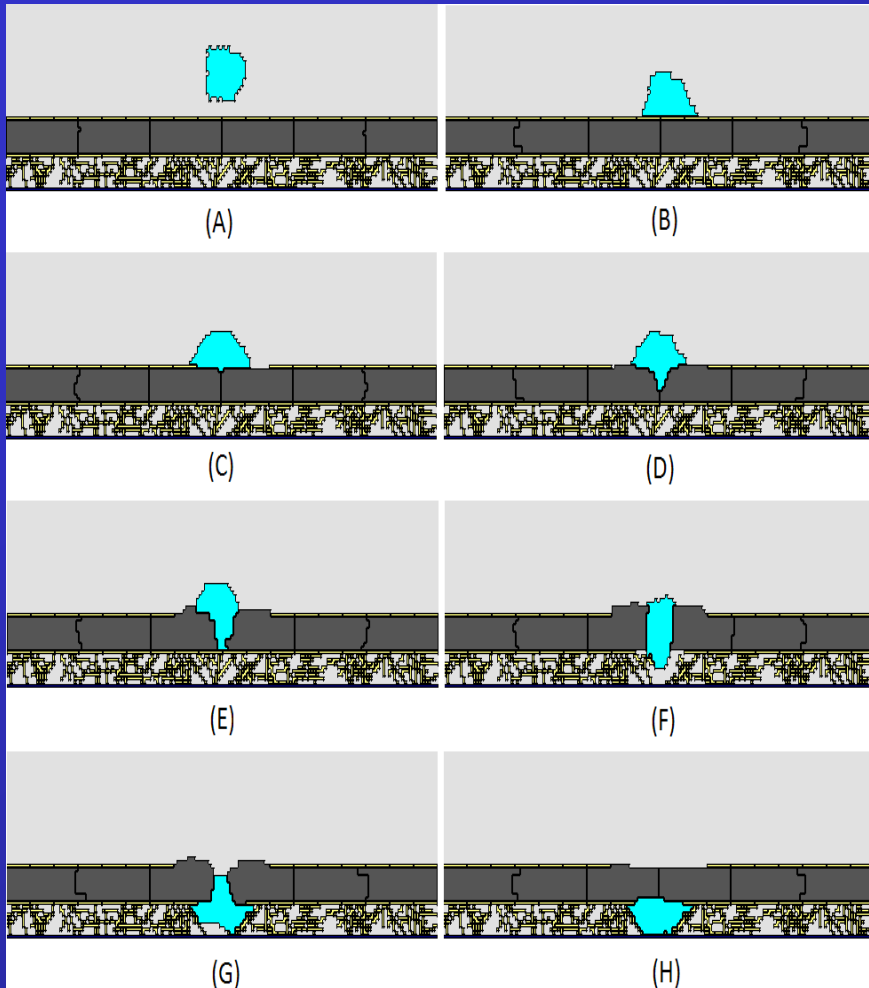
MATHEMATICAL MODEL



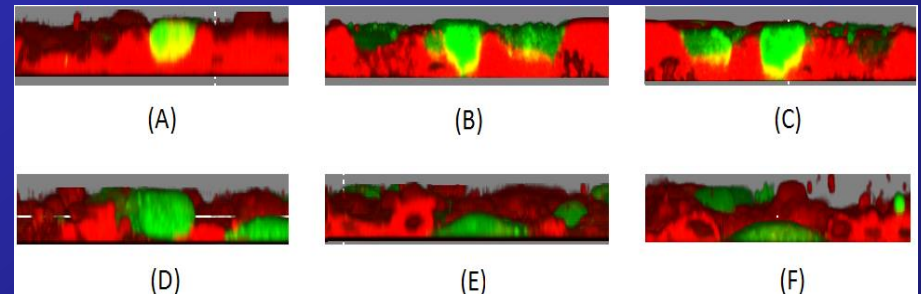
For example:

- ✓ the intracellular level of active cadherins or integrins will influence the cell-cell adhesion energy
- ✓ The level of extracellular growth factor will influence cell motility

APPLICATIONS



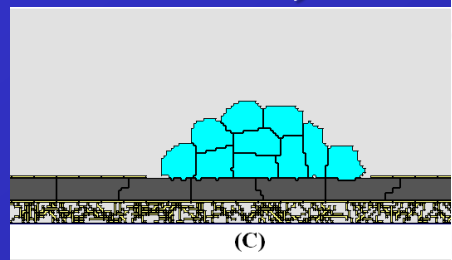
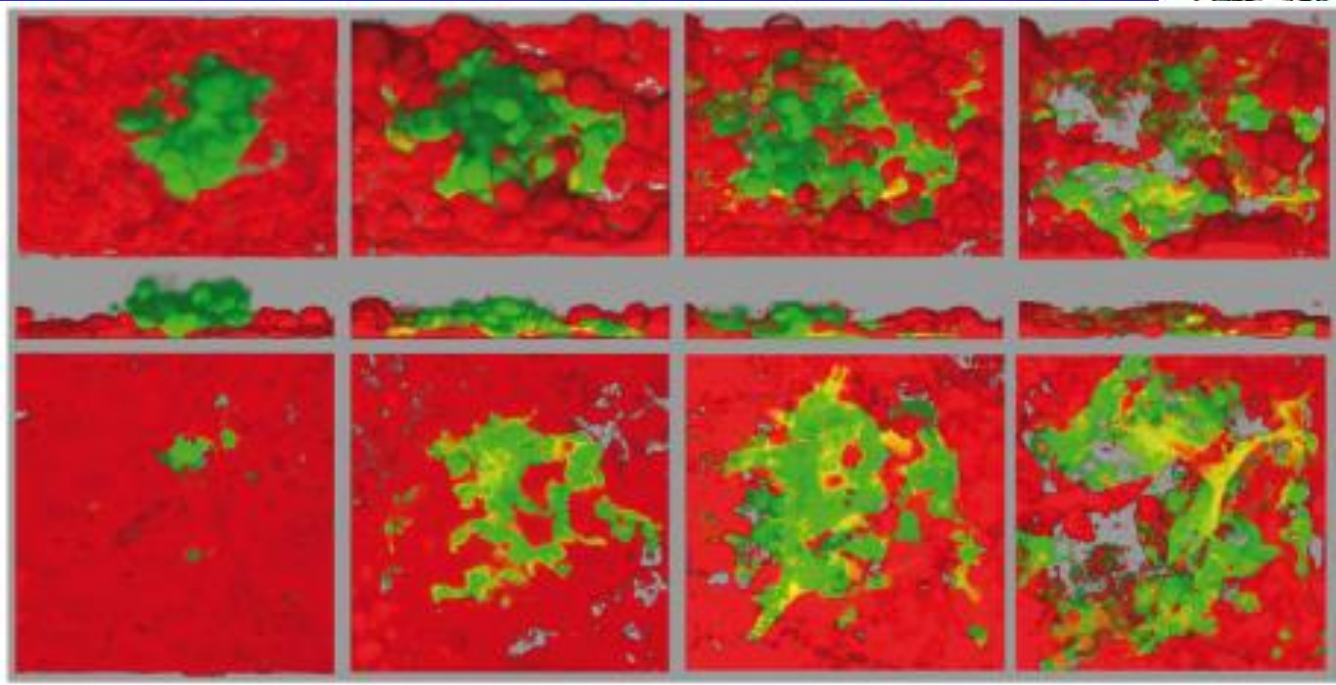
OVARIAN CANCER TRANS-MESOTHELIAL INVASION (with Prof. A. Funaro)



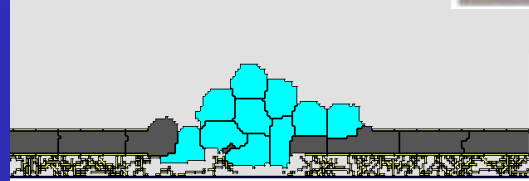
MS, Giverso, Lo Buono, Preziosi, Funaro,
Math Model Nat Phenom, 2010.

APPLICATIONS

OVARIAN CANCER TRANS- MESOTHELIAL INVASION (with Prof. A. Funaro)



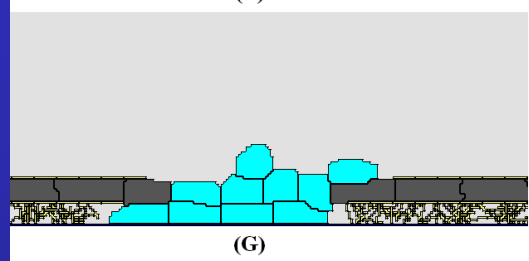
(C)



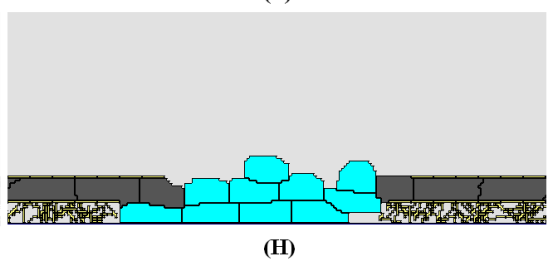
(E)



(F)



(G)

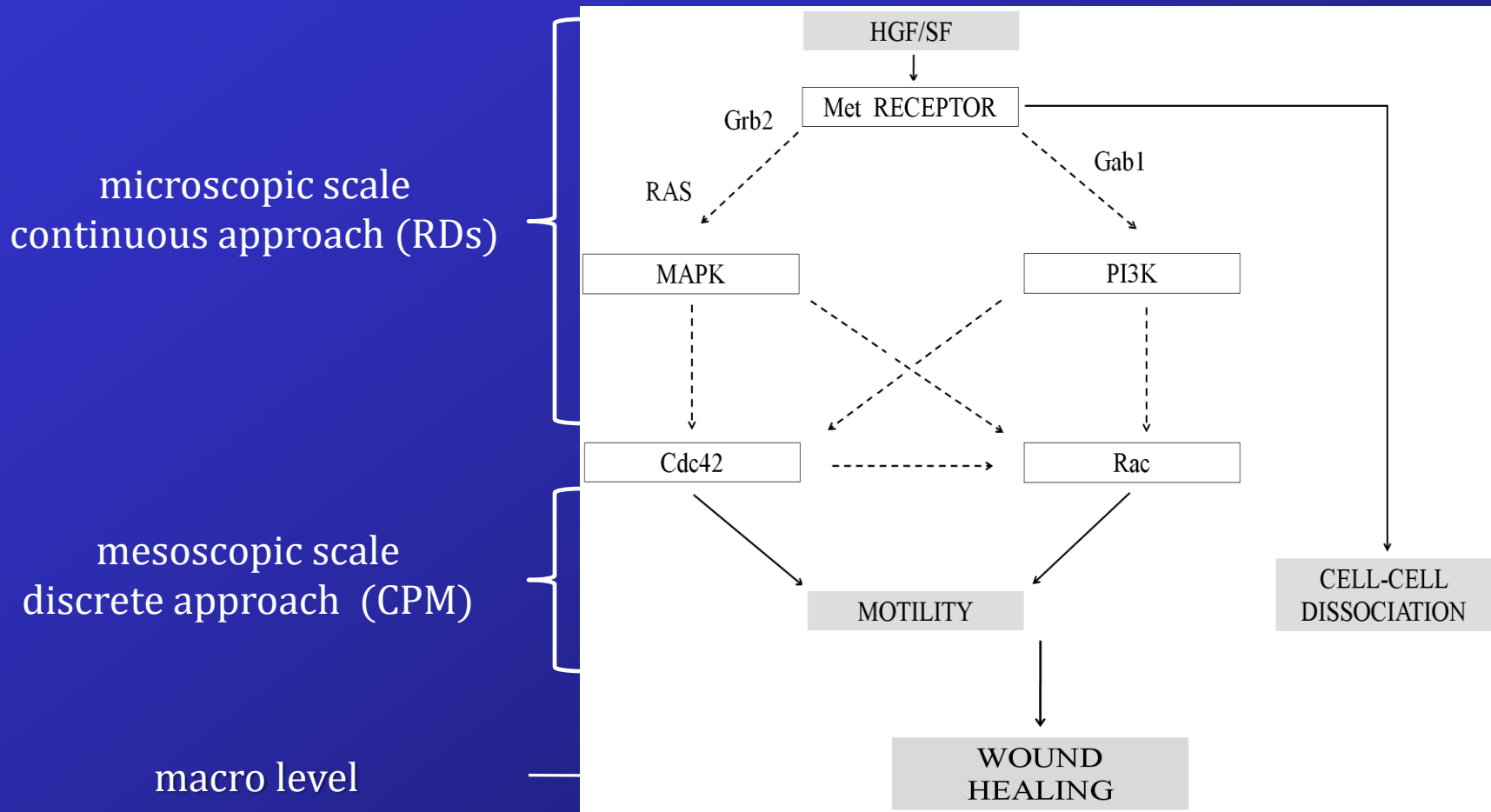


(H)

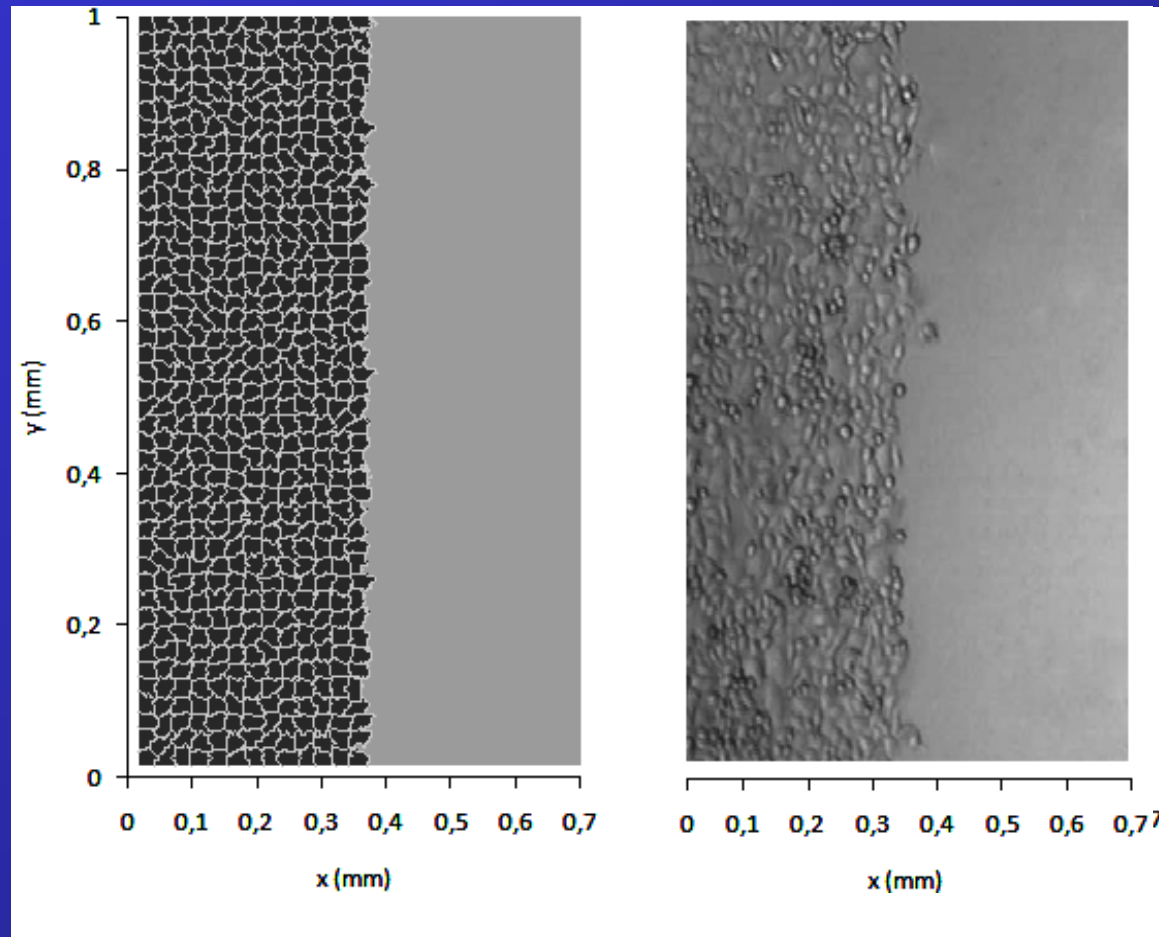
MS, Giverso, Lo
Buono, Preziosi,
Funaro, Math
Model Nat Phenom,
2010.



WOUND HEALING ASSAY OF EPITHELIAL CELLS IN RESPONSE TO A MOTILITY FACTOR (i.e., HGF)

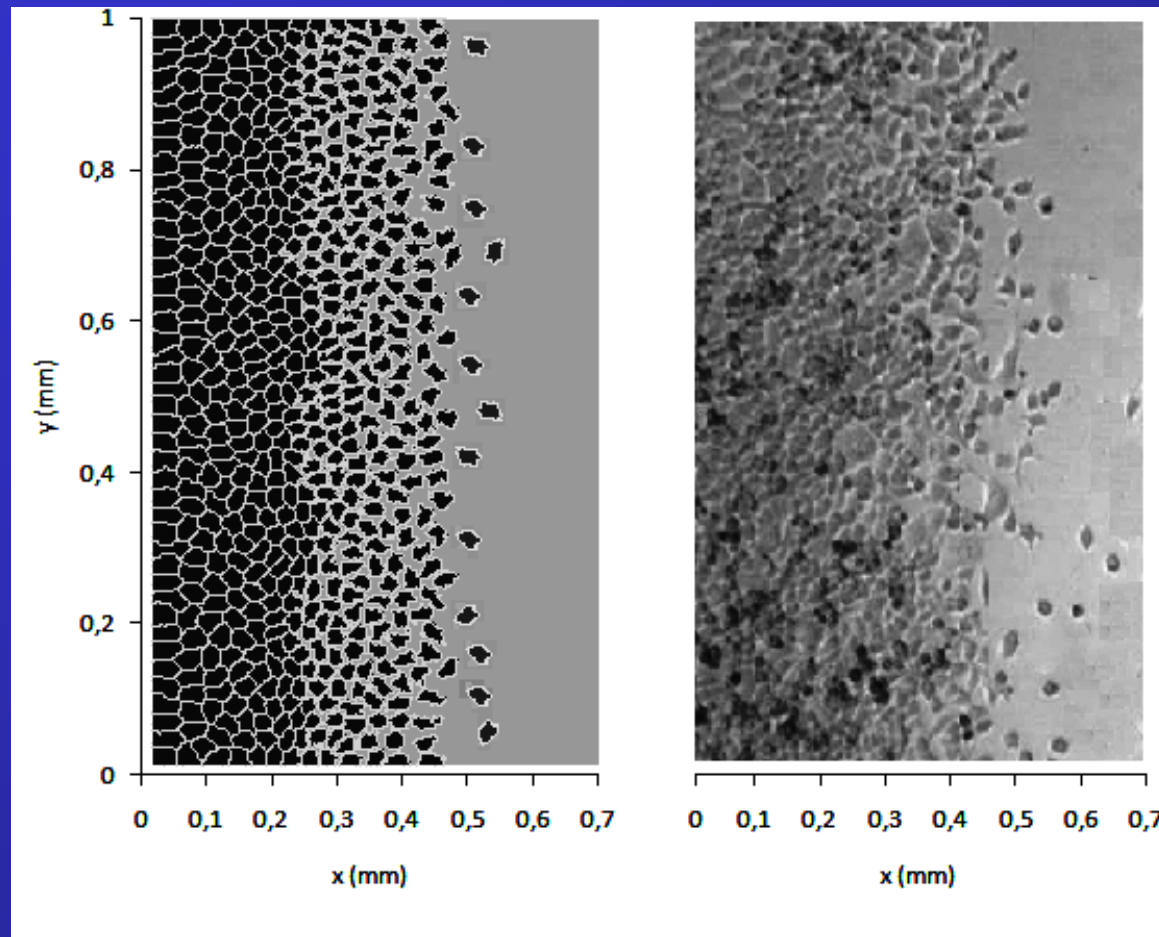


WOUND HEALING ASSAY OF EPITHELIAL CELLS IN RESPONSE TO A MOTILITY FACTOR (i.e., HGF)



$t = 0$ h

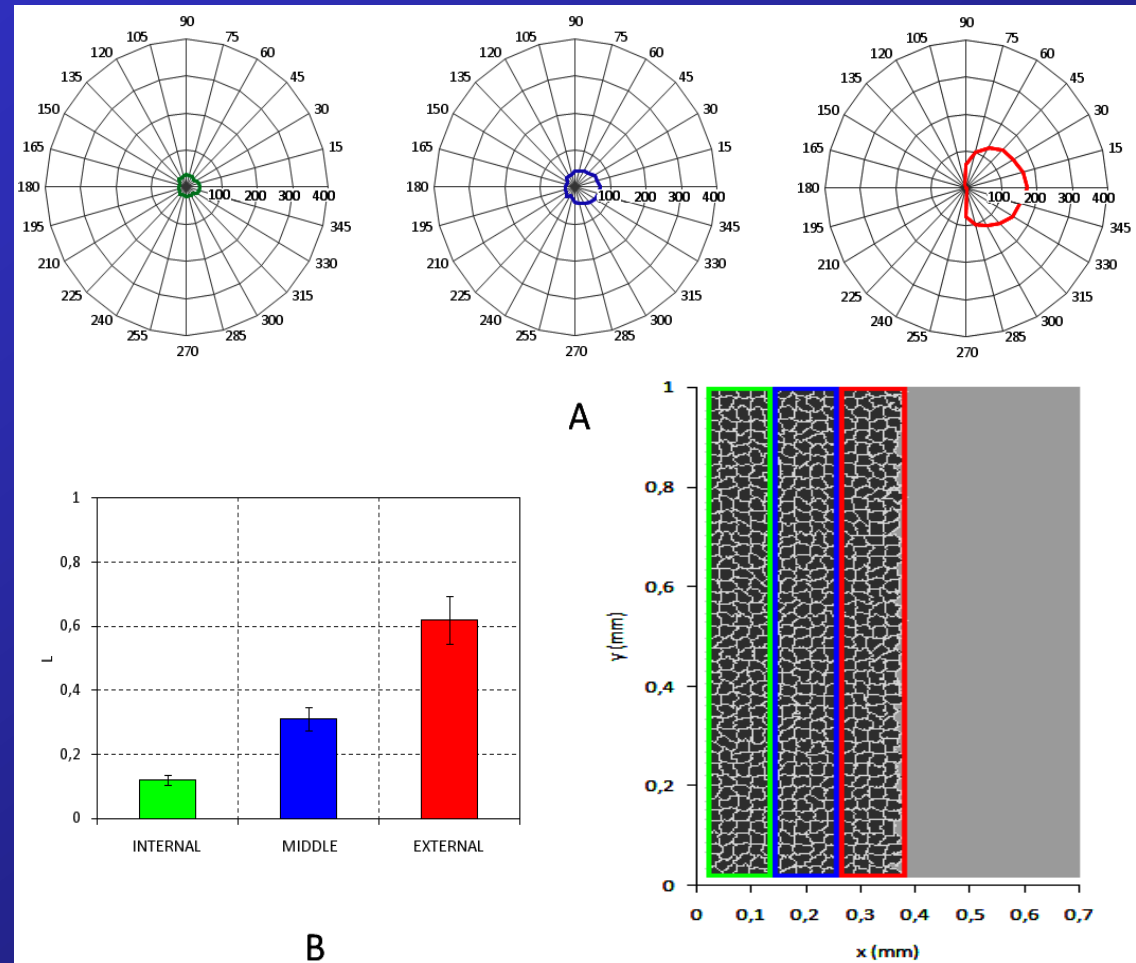
WOUND HEALING ASSAY OF EPITHELIAL CELLS IN RESPONSE TO A MOTILITY FACTOR (i.e., HGF)



$t = 12$ h

WOUND HEALING ASSAY OF EPITHELIAL CELLS IN RESPONSE TO A MOTILITY FACTOR (i.e., HGF)

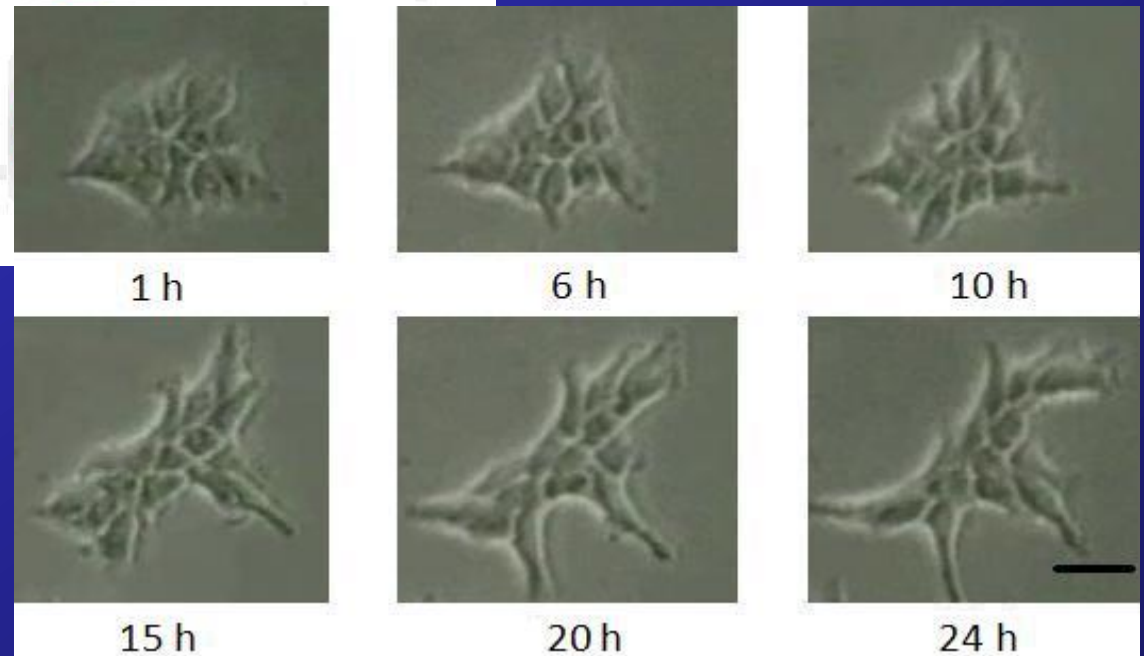
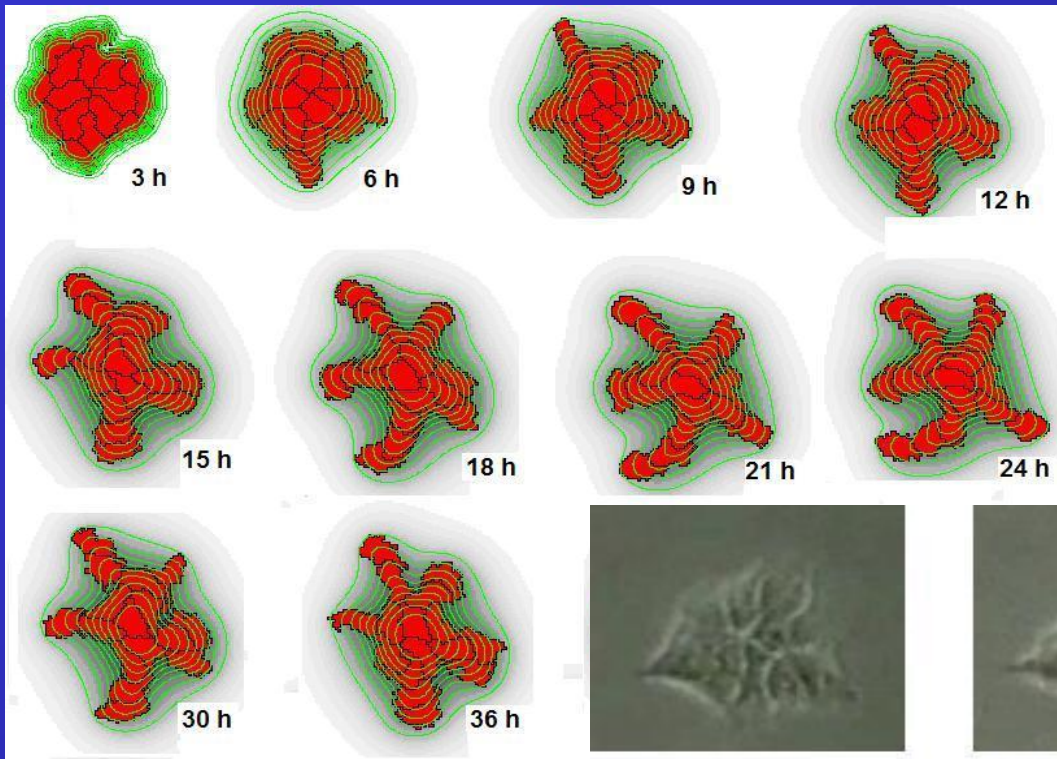
the cell mass can be sorted into three subpopulations, namely internal, middle and external, characterized by well-defined migratory behavior



APPLICATIONS



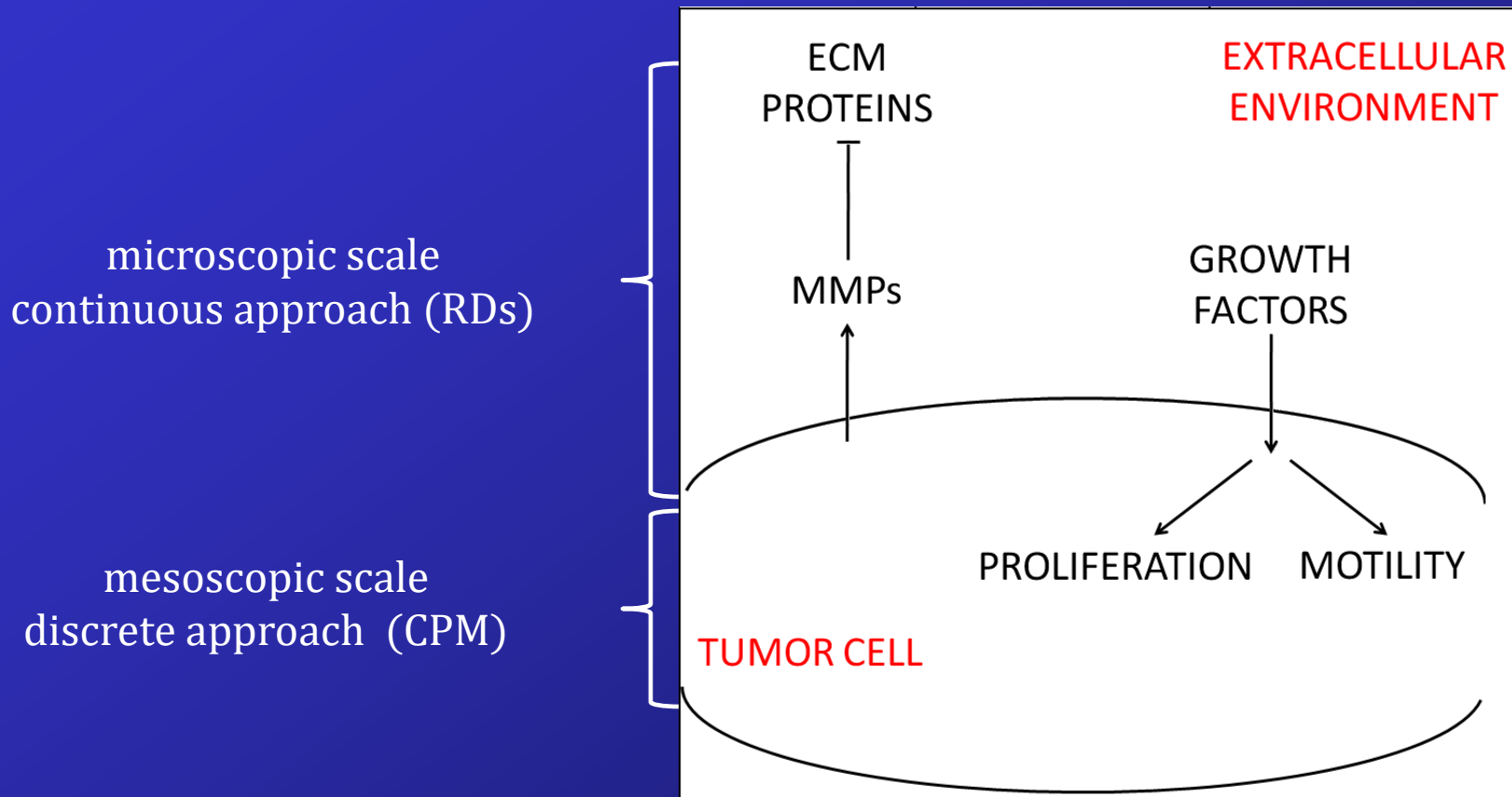
CELL SCATTERING OF
MLP-29 COLONIES IN
RESPONSE TO HGF/SF
(with Prof. E. Medico)



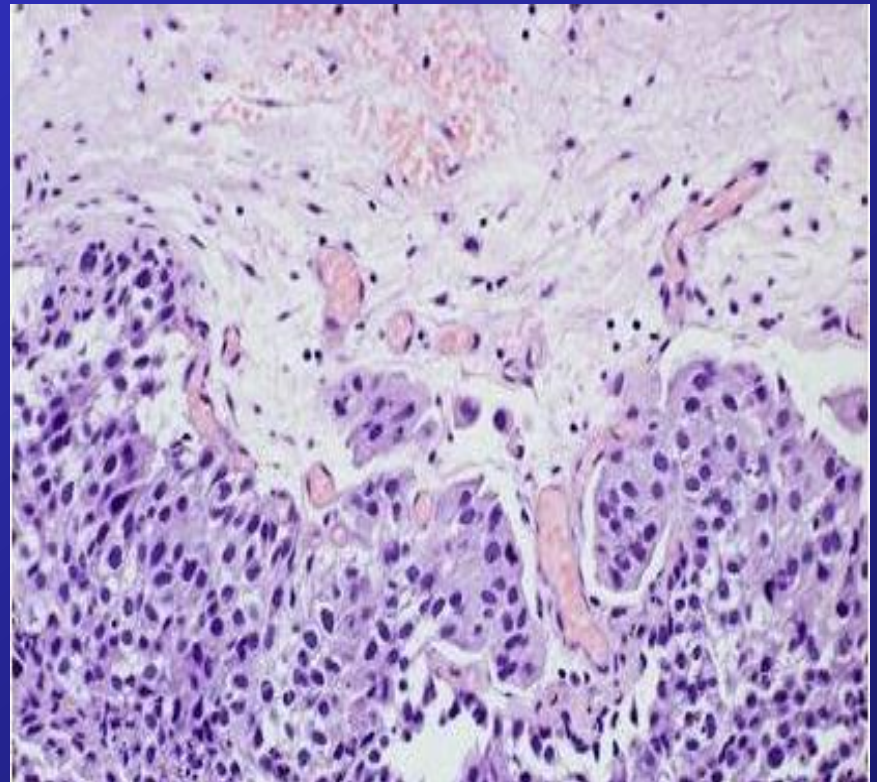
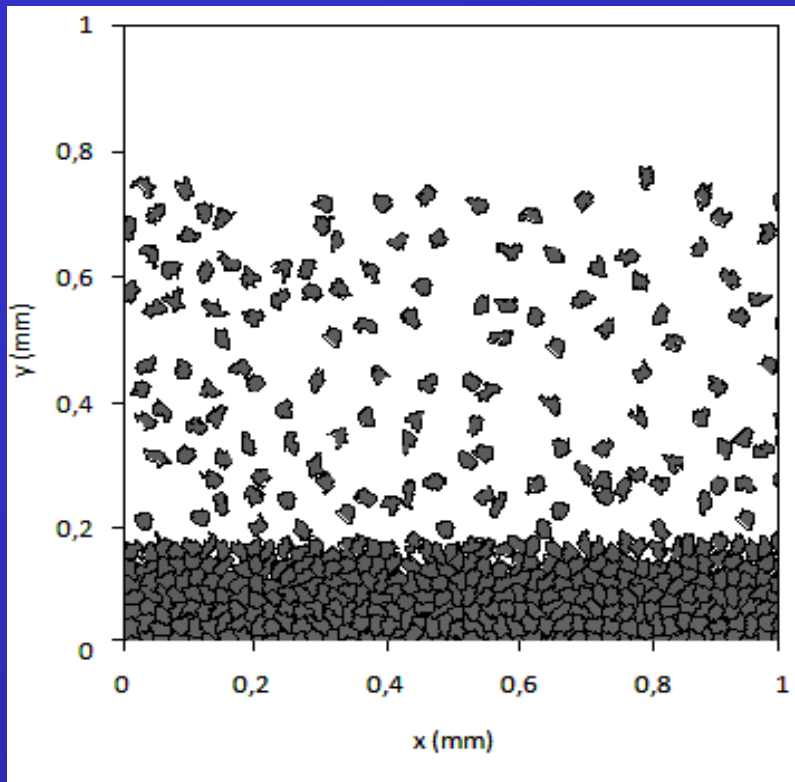
MS, Merks, Preziosi,
Medico, J Theor Biol, 2009.



DIFFERENT MORPHOLOGIES OF TUMOR INVASION FRONTS

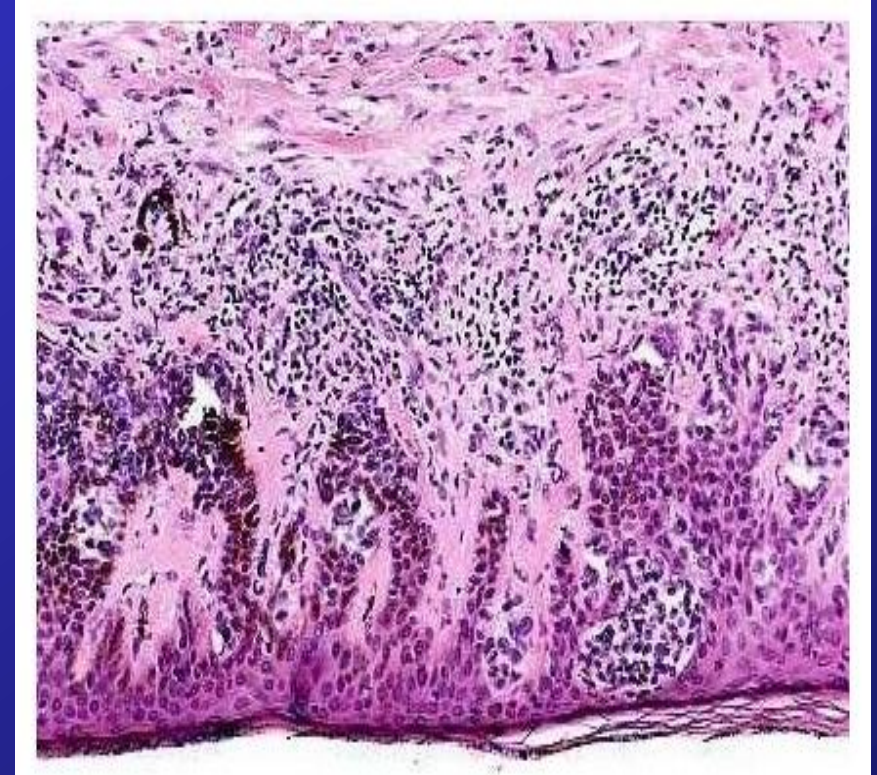
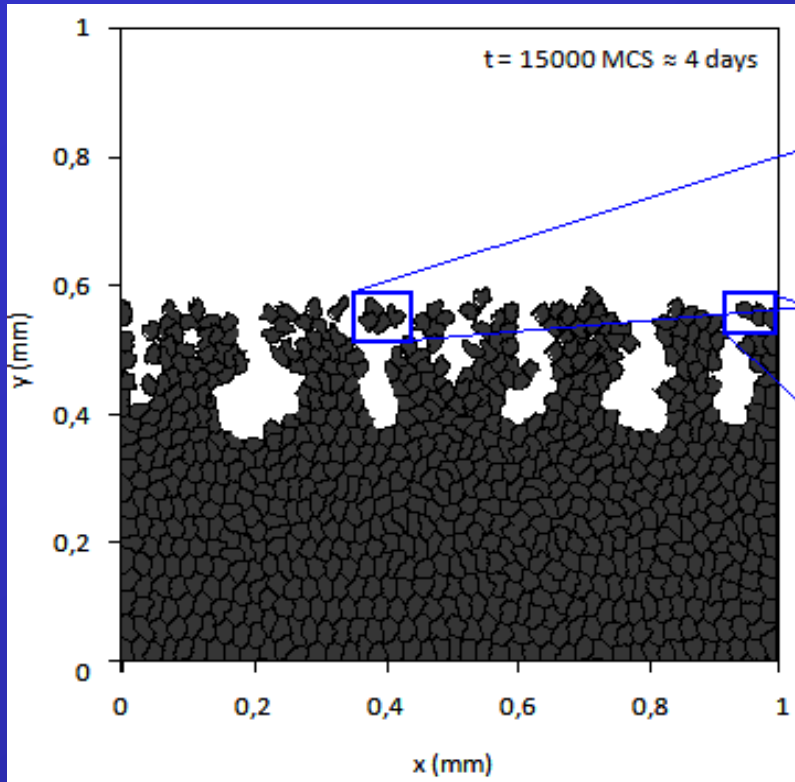


DIFFERENT MORPHOLOGIES OF TUMOR INVASION FRONTS



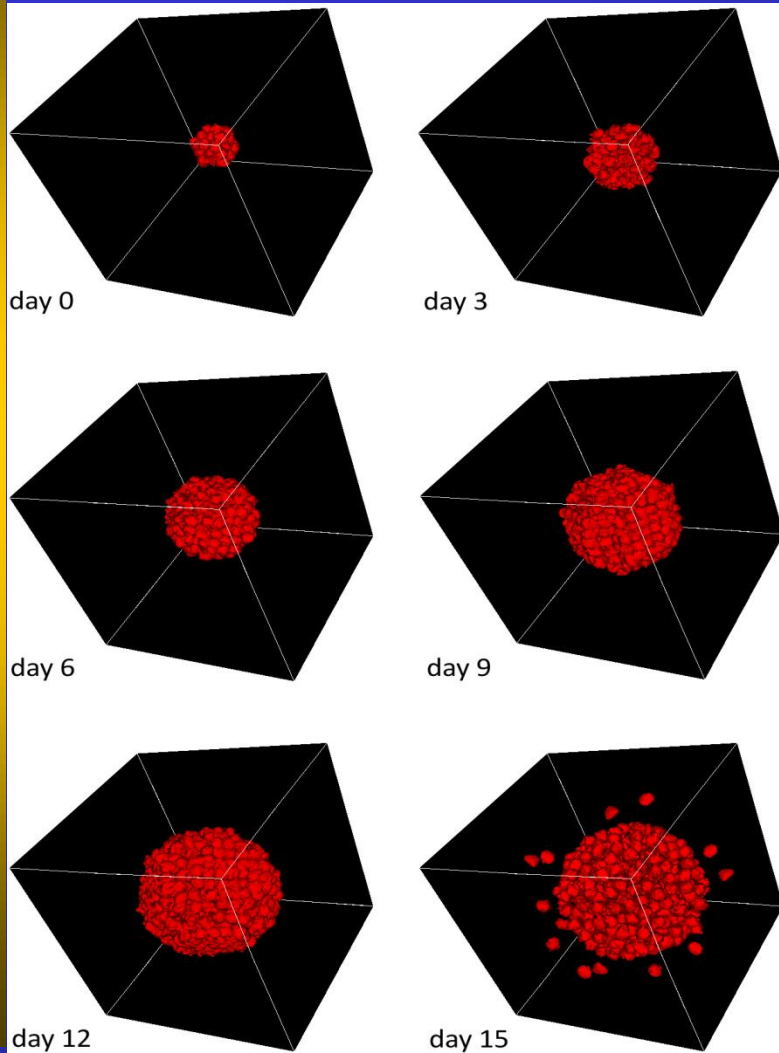
in silico and *in vivo* pT1 urothelial carcinoma invading into the lamina propria, with single aggressive malignant cells detaching from the main tumor mass

DIFFERENT MORPHOLOGIES OF TUMOR INVASION FRONTS

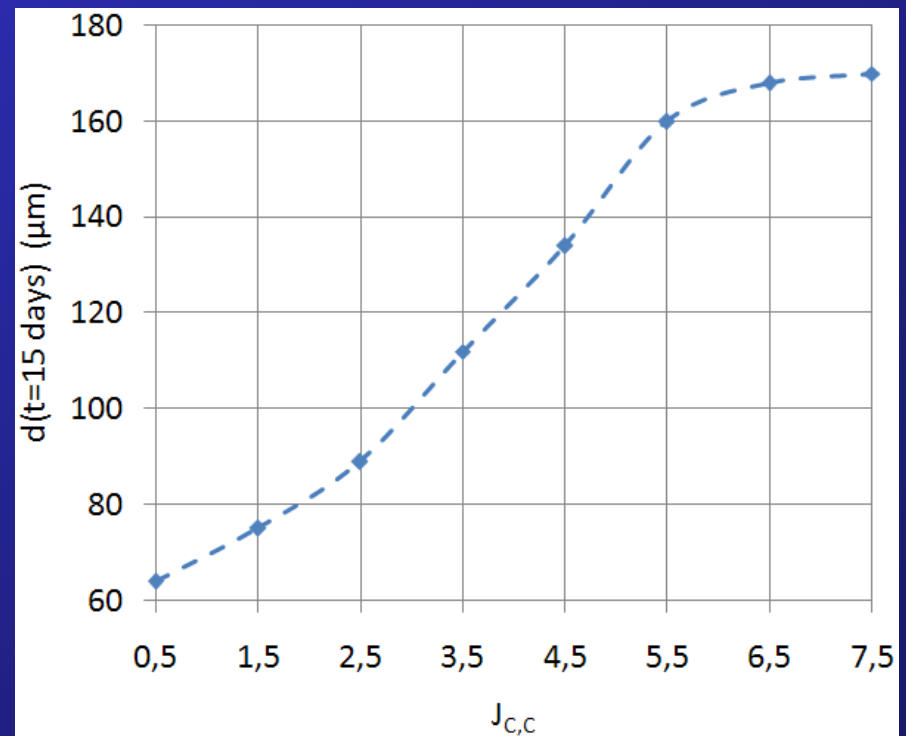


in silico and *in vivo* microinvasive tumor of the cervix, with fingers of invading cells protruding through the basement membrane

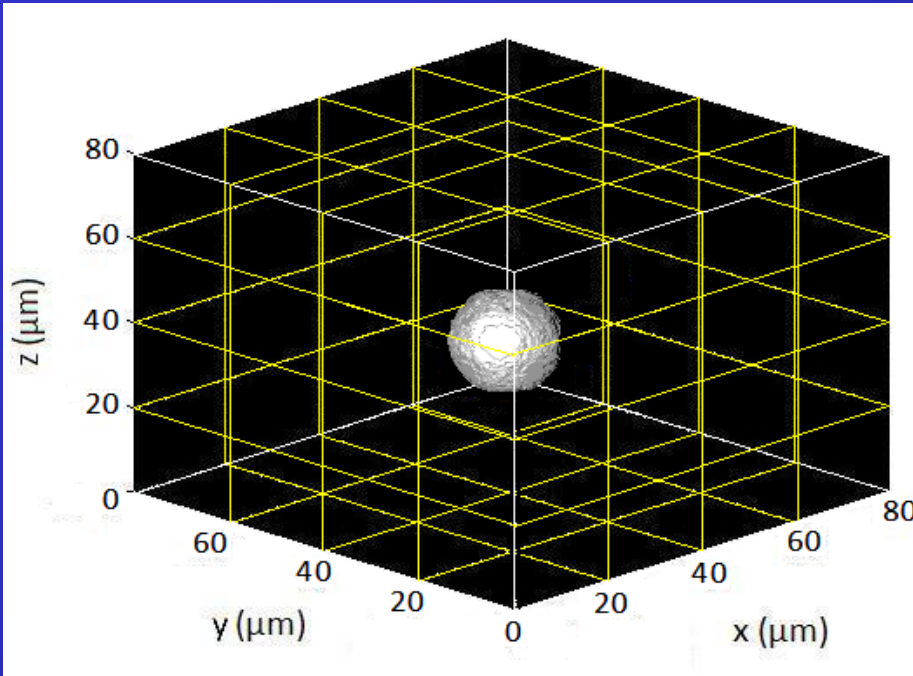
DIFFERENT MORPHOLOGIES OF TUMOR INVASION FRONTS



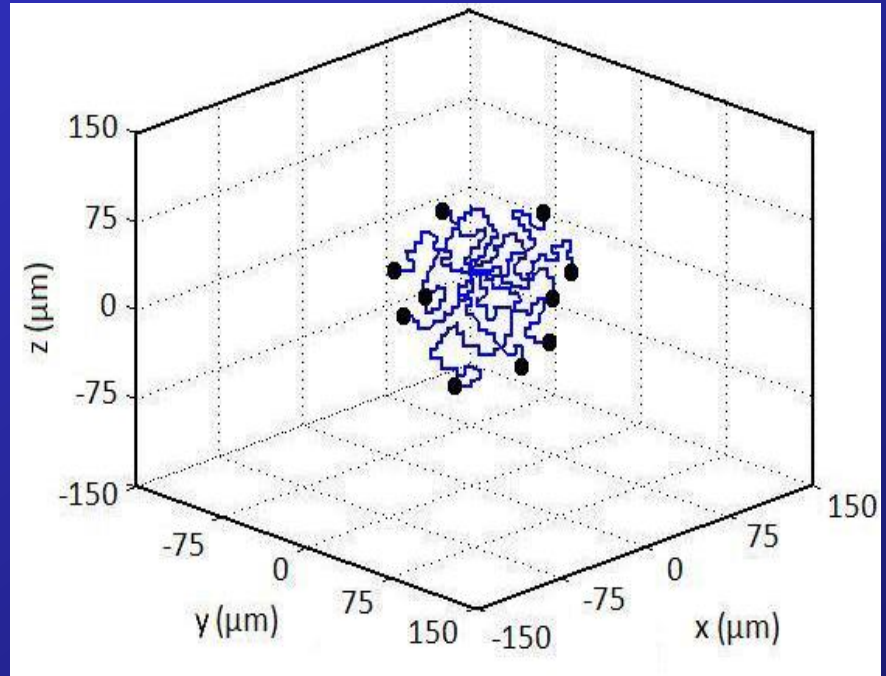
simulation of the evolution of a glioma spheroid. The tumor invasiveness is strictly regulated by intercellular adhesion



CELL MIGRATION IN 3D MATRIX SCAFFOLDS

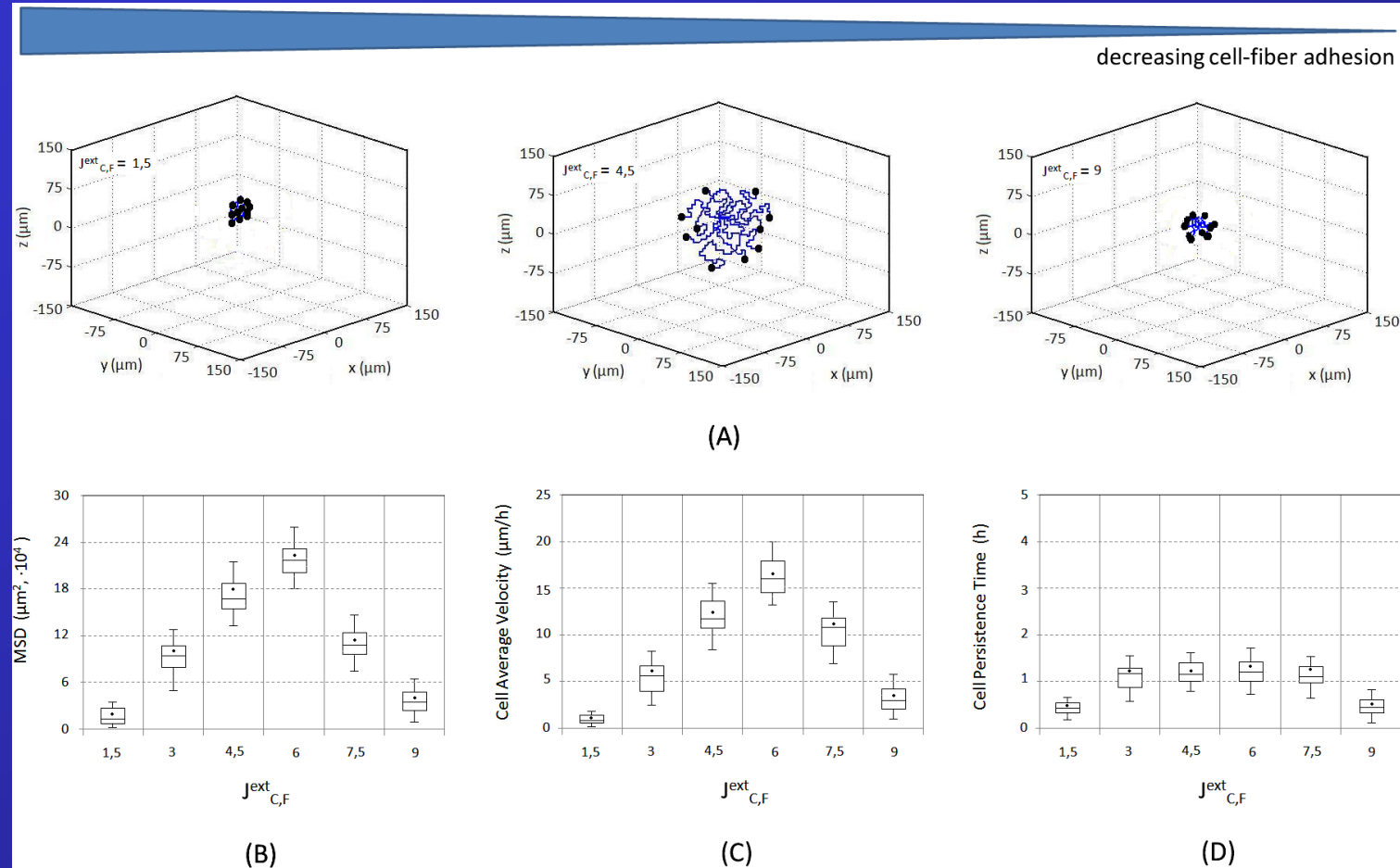


cells are seeded in an isotropic two-component matrix scaffold, characterized by a regular mesh of inelastic fibers with square pores



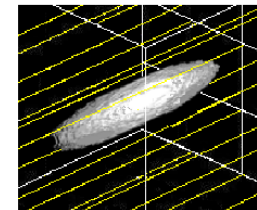
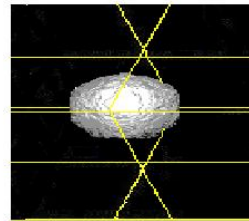
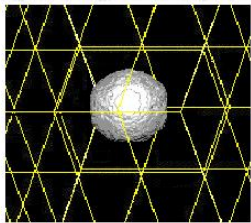
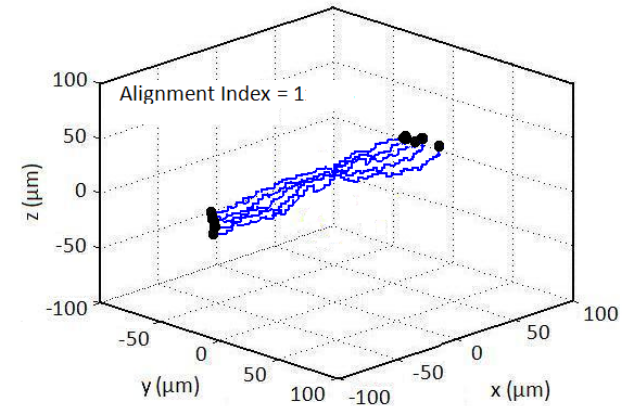
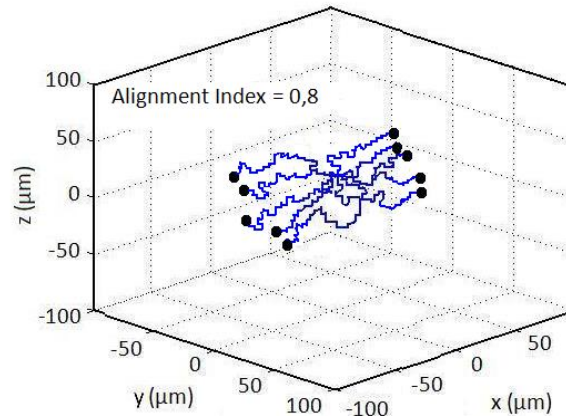
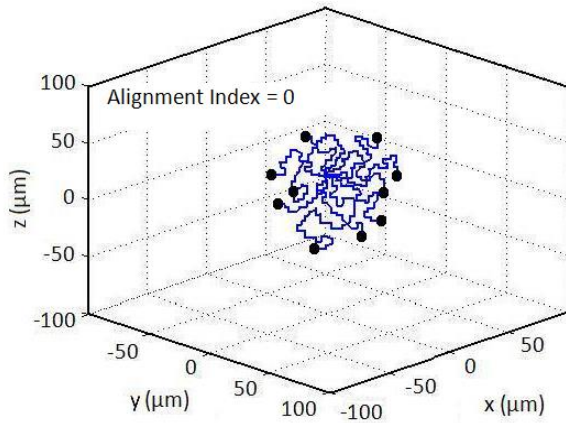
cell movement is Brownian with a mean net displacement of $75 \mu\text{m}$ in 12 h, a velocity of $14 \mu\text{m/h}$, and a persistence time less than 1.5 h

CELL MIGRATION IN 3D MATRIX SCAFFOLDS



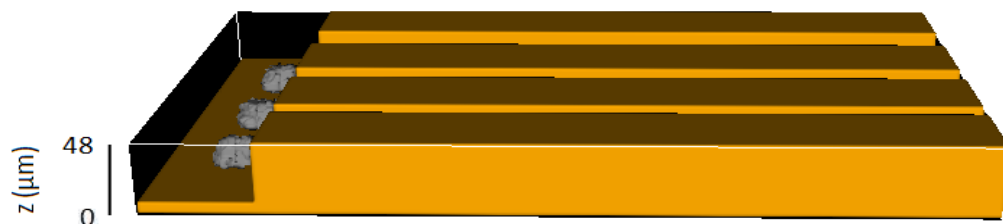
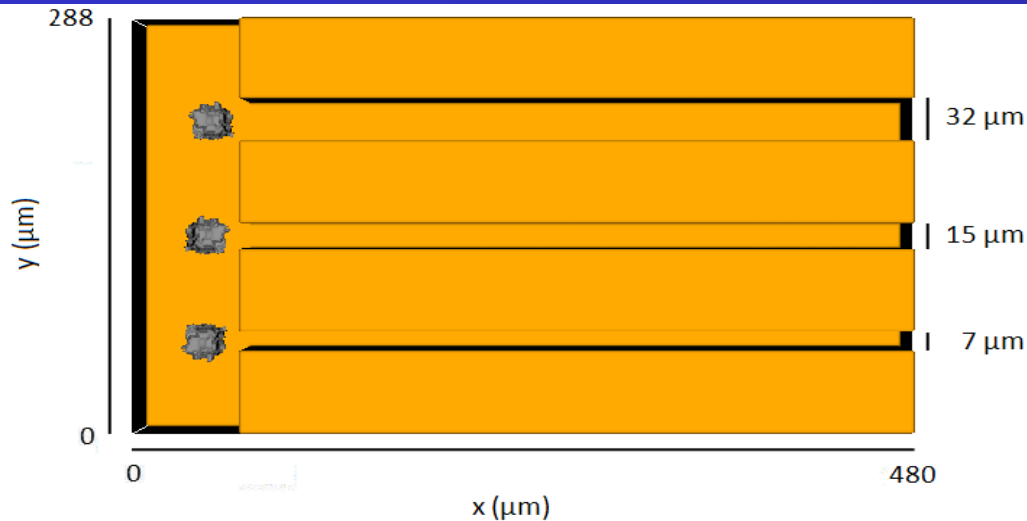
a bimodal relation is found between cell motile behavior and cell-fiber adhesion

CELL MIGRATION IN 3D MATRIX SCAFFOLDS



the directional component of cell motion increases until, in the case of all fibers aligned along the x-axis, cells movement is almost linear, with no change in cell velocity.

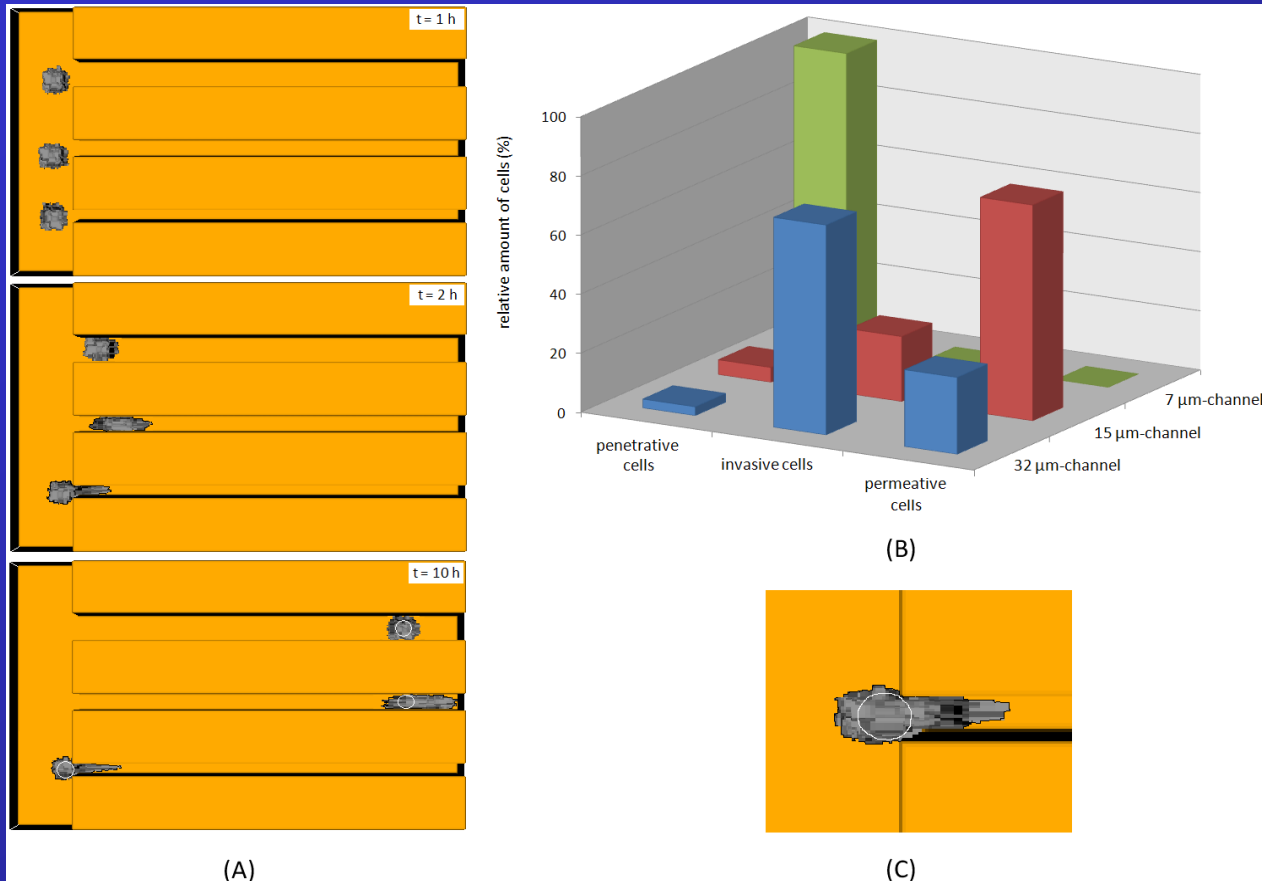
CELL MIGRATION IN 3D MICROCHANNELS



bottom channel size < nucleus diameter < middle channel size < cell diameter < top channel size

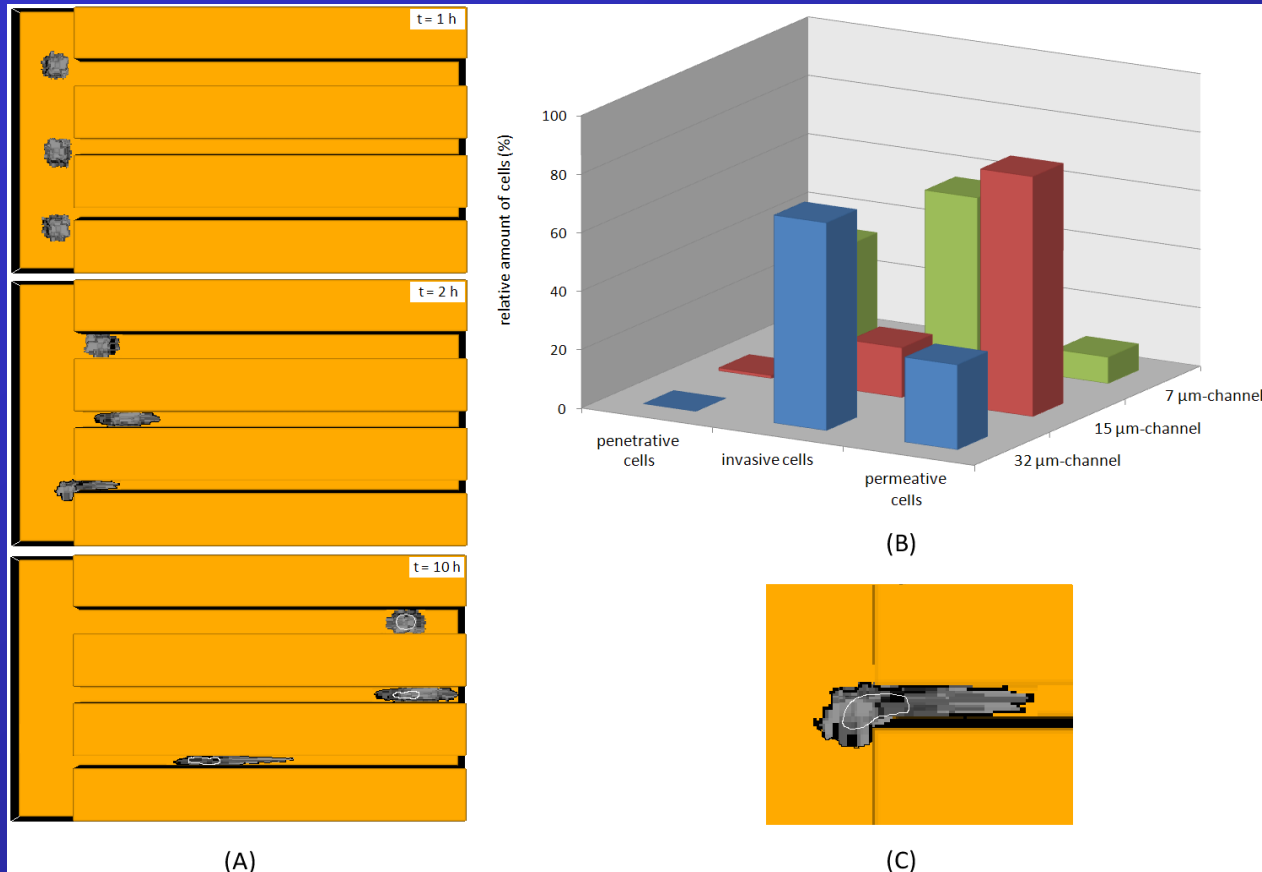
The model reproduces a micro-fabricated device with channels of various width and a planar surface just outside their entrance. The cell migratory behavior is characterized by one of the following categories: i) cells that only penetrate the channel with a part of their cytoplasm are classified as penetrating, ii) cells that completely enter in the channel structure but are not able to migrate to the other side within the observation period are called invasive, iii) cells that reach the opposite border of the channel are finally termed permeative.

CELL MIGRATION IN 3D MICROCHANNELS



Migratory behavior of cells with an elastic cytosol and a still rigid nucleus. They are now able to enter also in the intermediate channel, displaying a permeative behavior. However, they are constrained to stay outside the smaller structure.

CELL MIGRATION IN 3D MICROCHANNELS

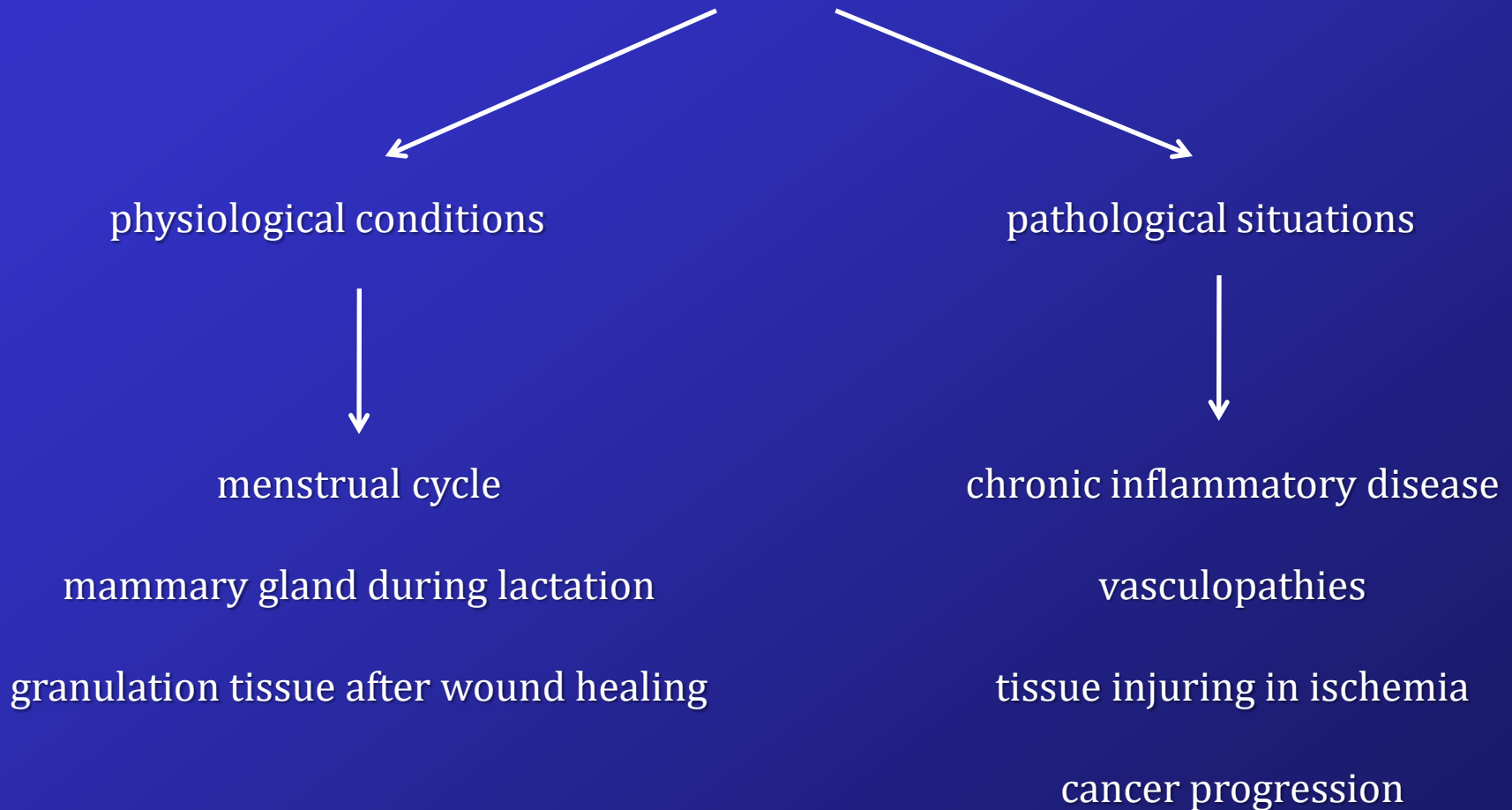


Migratory behavior of cells with an elastic cytosol and a deformable nucleus. The enhancement in nucleus elasticity enables cells to enter also in the smallest channel, where they acquire an invasive phenotype



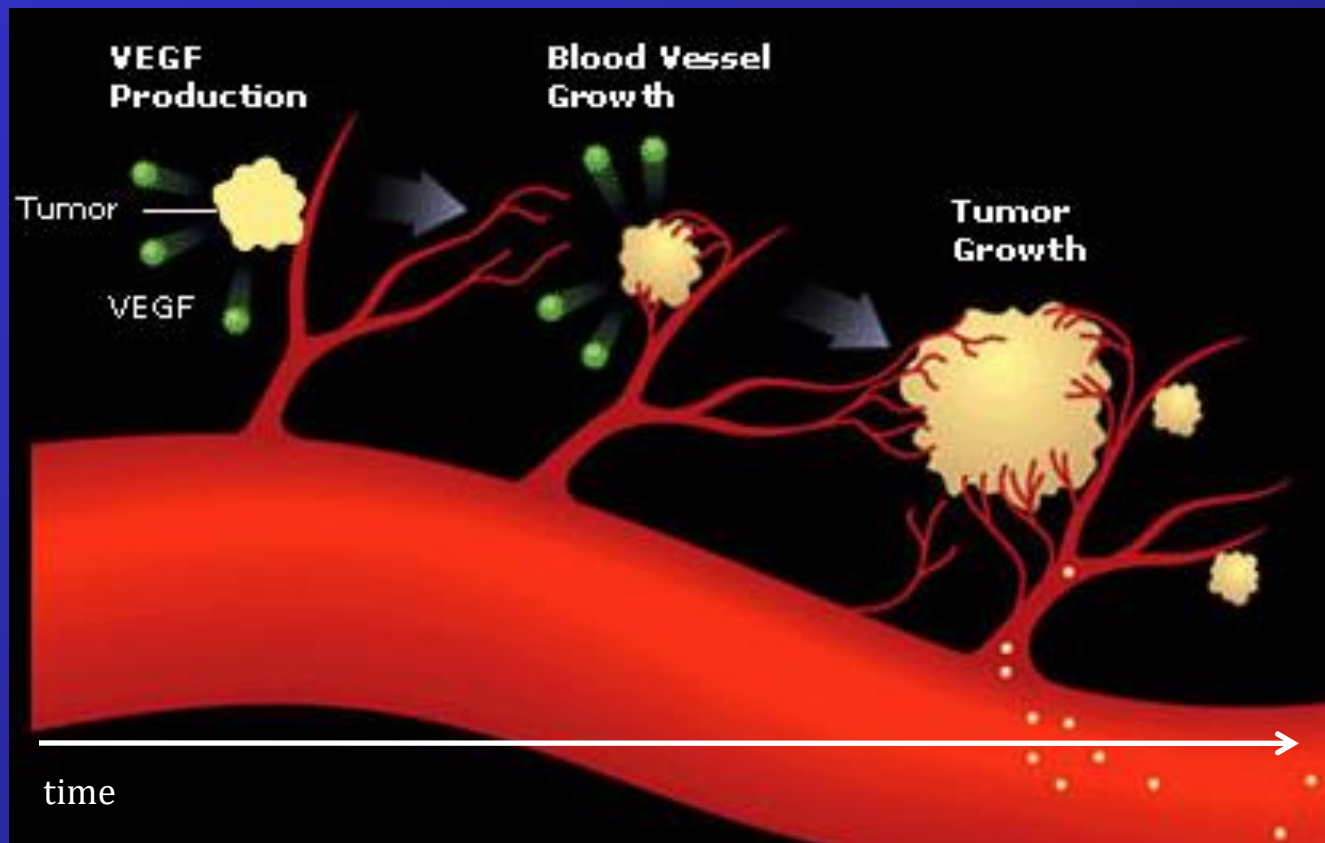
APPLICATIONS: TUMOR-DERIVED VASCULOGENESIS

Blood vessel formation is a complex and multilevel process fundamental in:



APPLICATIONS: TUMOR-DERIVED VASCULOGENESIS

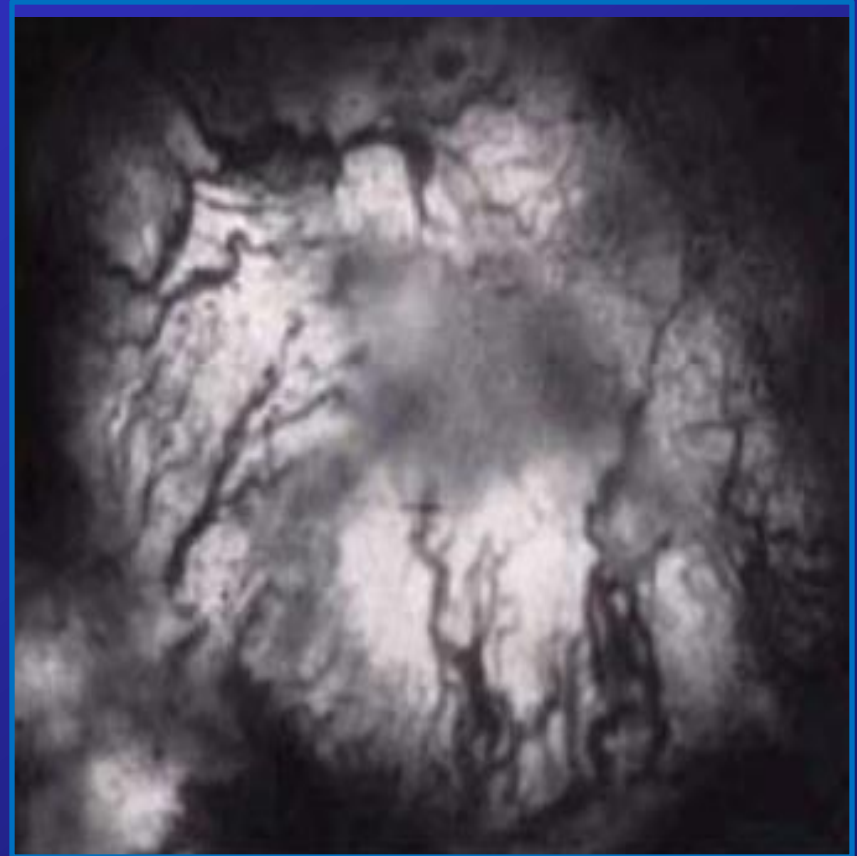
Vascularization is a pivotal step in tumor development, providing the necessary nutrients and allowing malignant cells enter in the circulatory system



APPLICATIONS: TUMOR-DERIVED VASCULOGENESIS



The discovery of efficient anti-angiogenic therapies is a fundamental issue in cancer research and treatment has given rise to multiple experiments, which aim to understand the key mechanisms involved in malignant vascularization and to identify intervention strategies potentially able to disrupt them



Experimental image of a vascularized solid tumor, courtesy of the Institute for Cancer Research and Treatment, Candiolo, Italy



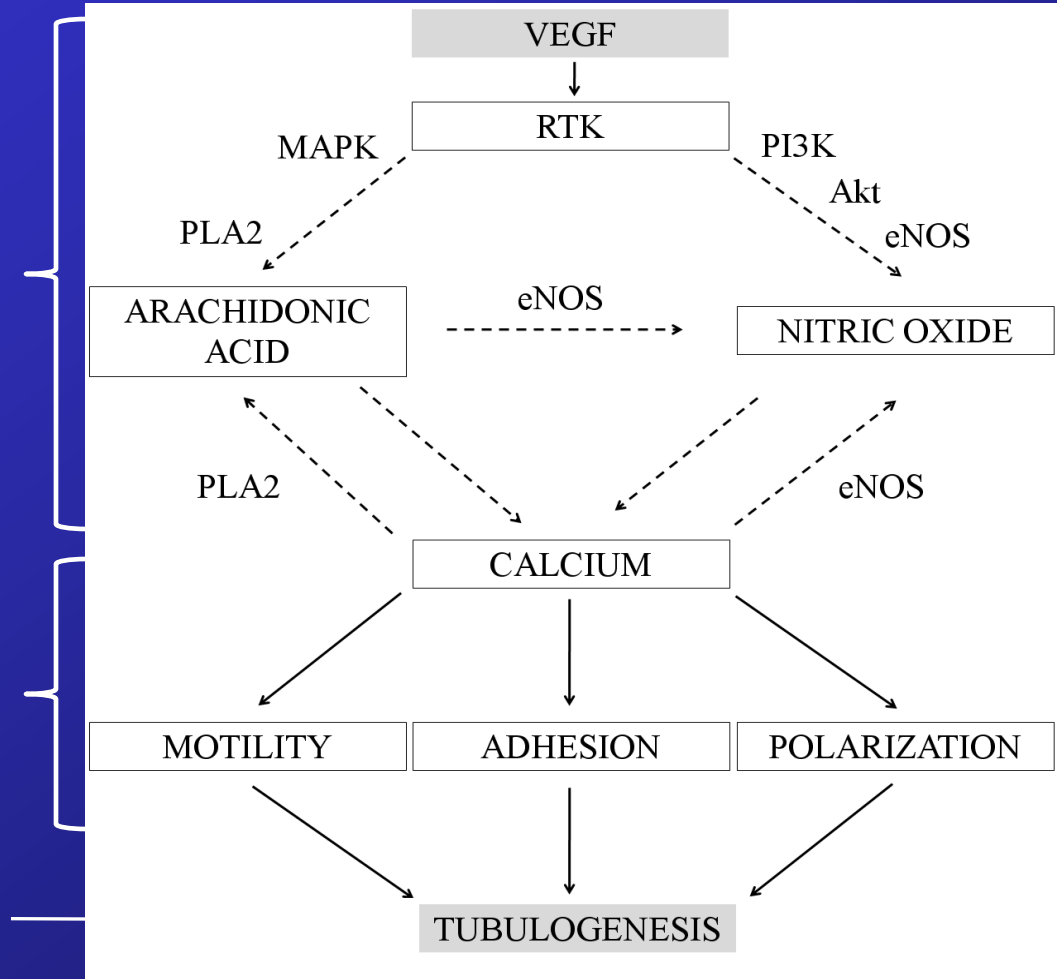
APPLICATIONS: TUMOR-DERIVED VASCULOGENESIS

(with Prof. L. Munaron)

microscopic scale
continuous approach (RDs)

mesoscopic scale
discrete approach (CPM)

macro level





APPLICATIONS: TUMOR-DERIVED VASCULOGENESIS

The system of equations regulating the intracellular biochemical pathways is given as

Extracellular VEGF

$$\frac{\partial h_{\text{VEGF}}}{\partial t} = \underbrace{D_{\text{VEGF}} \frac{\partial^2 h_{\text{VEGF}}}{\partial x^2}}_{\text{diffusion}} - \underbrace{k_{\text{VEGF}} h_{\text{VEGF}}}_{\text{decay}} - \underbrace{y_{\text{VEGF}} h_{\text{VEGF}}}_{\text{cell uptake}} + \underbrace{s_{\text{VEGF}}}_{\text{addition}}$$

Intracellular messengers

$$\frac{\partial h_{\text{AA}}}{\partial t} = \underbrace{D_{\text{AA}} \frac{\partial^2 h_{\text{AA}}}{\partial x^2}}_{\text{diffusion}} - \underbrace{k_{\text{AA}} h_{\text{AA}}}_{\text{decay}} + \underbrace{j_{\text{AA}} \text{ VEGFR}}_{\text{VEGF-induced production}} + \underbrace{c_{\text{AA}} \text{ Ca}}_{\text{Ca-induced synthesis}}$$

$$\frac{\partial h_{\text{NO}}}{\partial t} = \underbrace{D_{\text{NO}} \frac{\partial^2 h_{\text{NO}}}{\partial x^2}}_{\text{diffusion}} - \underbrace{k_{\text{NO}} h_{\text{NO}}}_{\text{decay}} + \underbrace{j_{\text{NO}} \text{ VEGFR}}_{\text{VEGF-induced production}} + \underbrace{c_{\text{NO}} \text{ Ca}}_{\text{Ca-induced synthesis}} + \underbrace{b_{\text{AA}} h_{\text{AA}}}_{\text{AA-induced synthesis}}$$

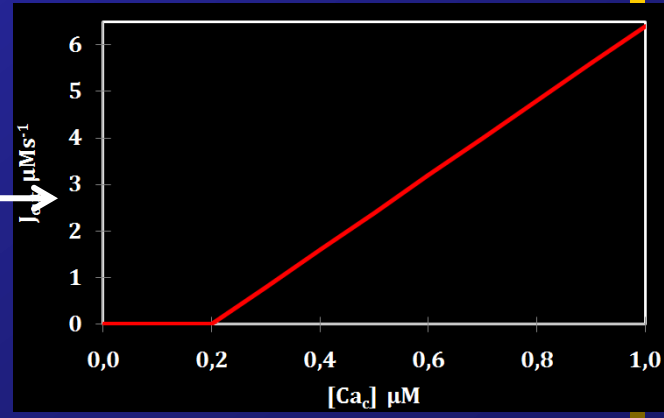
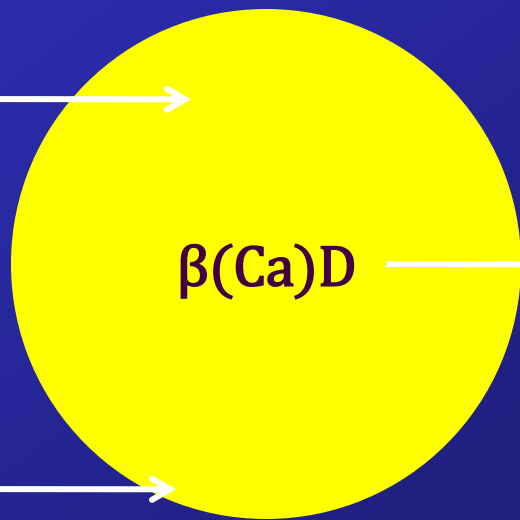
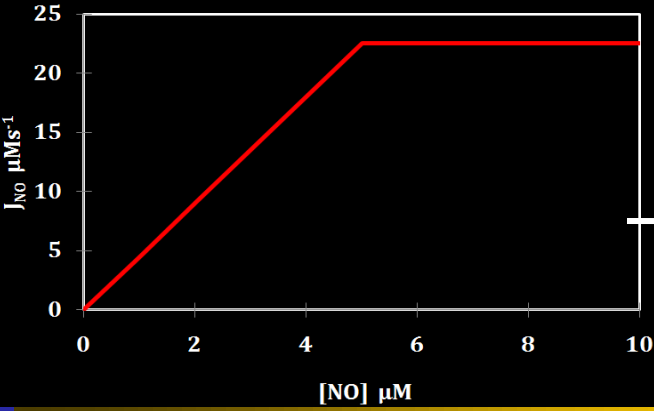
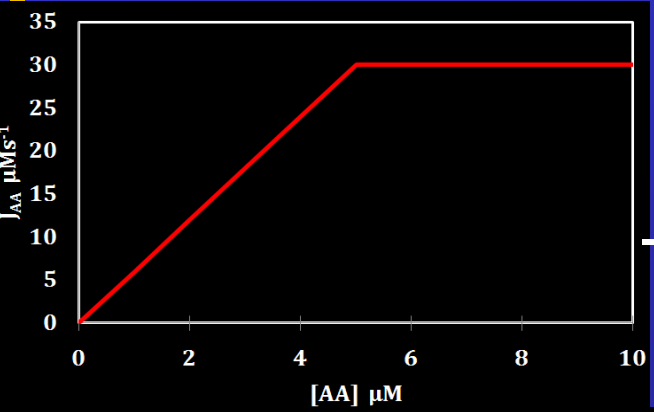


APPLICATIONS: TUMOR-DERIVED VASCULOGENESIS

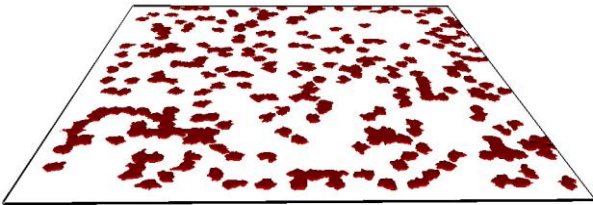
Intracellular calcium

$$\partial Ca / \partial t = \boxed{\beta(Ca) D \partial^2 Ca / \partial x^2} + \boxed{J_{AA} + J_{NO}} - \boxed{J_{out}}$$

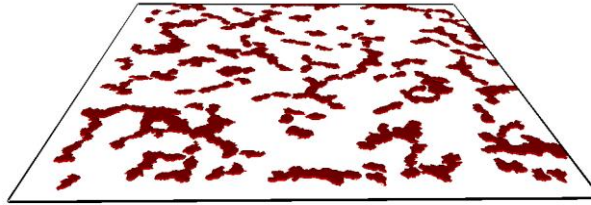
buffered diffusion AA- and NO-dependent influxes efflux



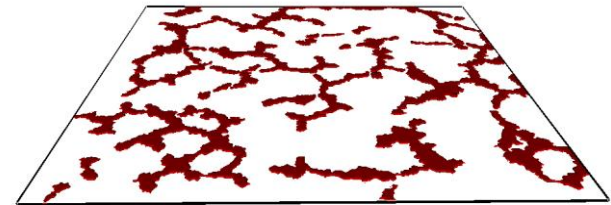
APPLICATIONS: TUMOR-DERIVED VASCULOGENESIS



(A)

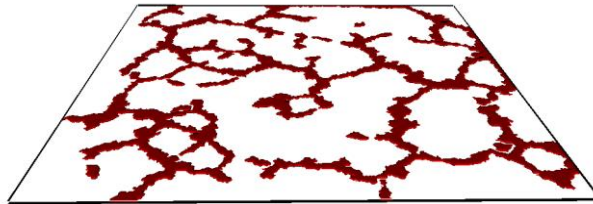


(B)

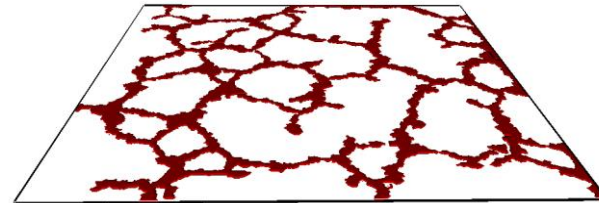


(C)

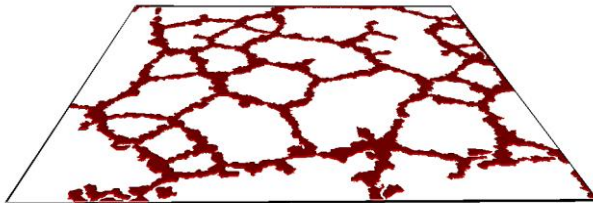
50 px \approx 50 μ m



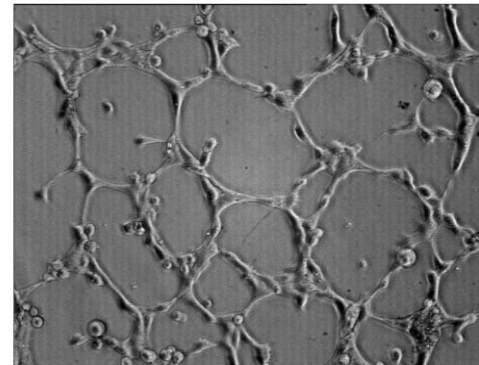
(D)



(E)



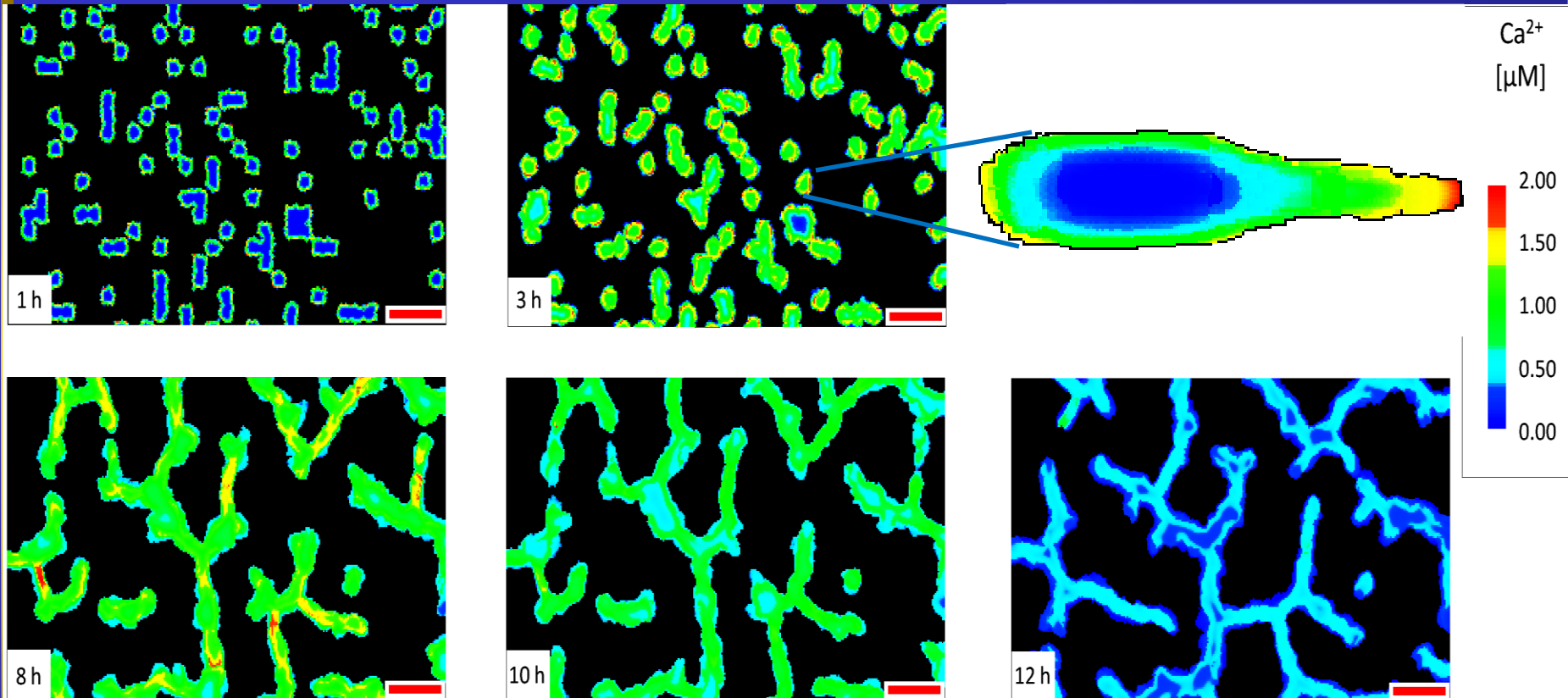
(F)



(G)

APPLICATIONS: TUMOR-DERIVED VASCULOGENESIS

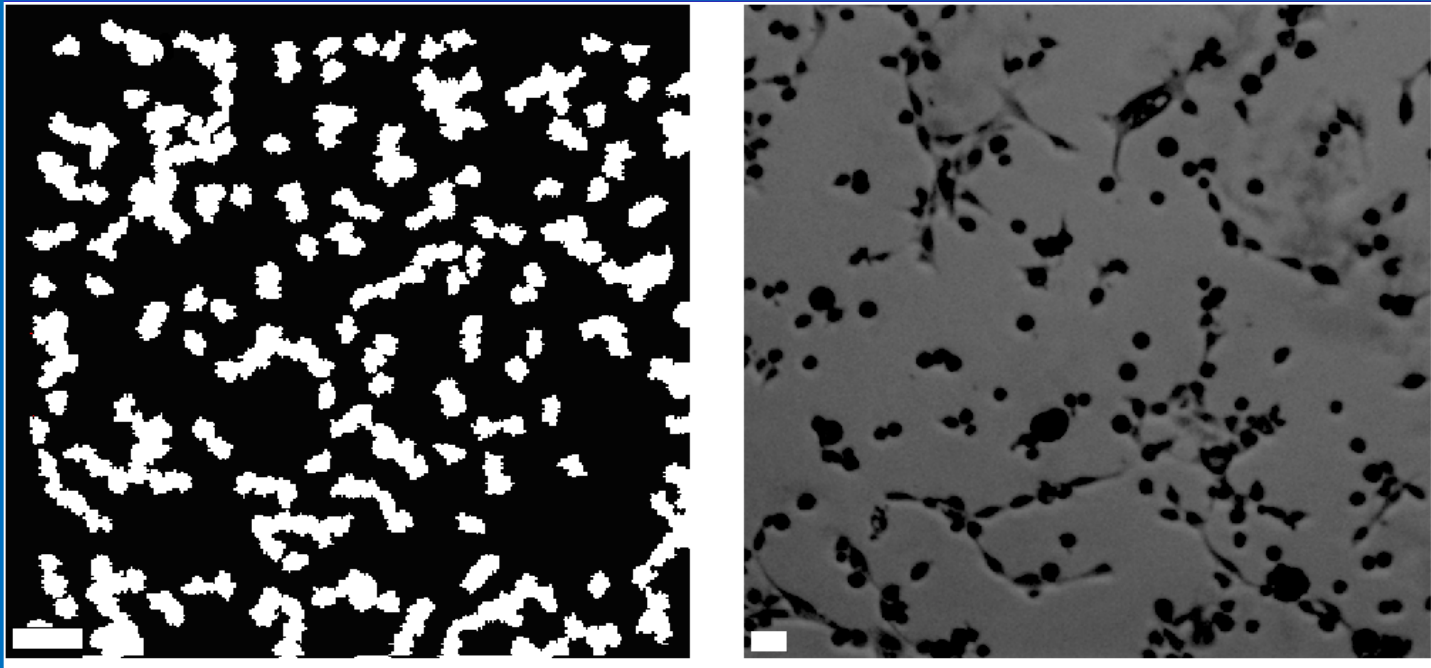
Evolution of intracellular calcium level during tubulogenesis



calcium signals, which are typically peripheral restricted, are detectable in the initial phase of the process, while they are down regulated during the maturation of EC tubules. The initial increment of calcium levels is in fact necessary for the enhancement of cell migratory properties

APPLICATIONS: TUMOR-DERIVED VASCULOGENESIS

Inhibition of calcium entry: carboxyamidotriazole, CAI, compound

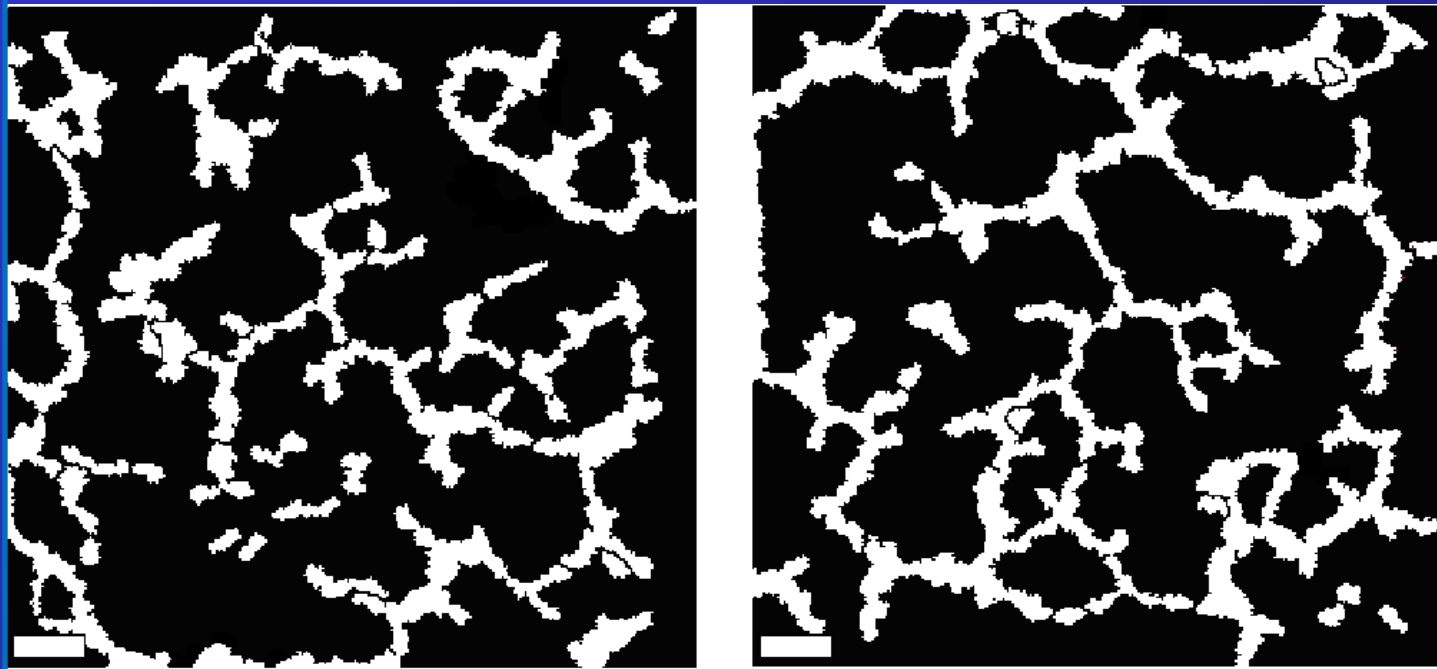


Experimental image courtesy of LM and of the Department of Animal and Human Biology, Università degli Studi di Torino.

complete disruption of tubule formation, as the TECs remain almost scattered

APPLICATIONS: TUMOR-DERIVED VASCULOGENESIS

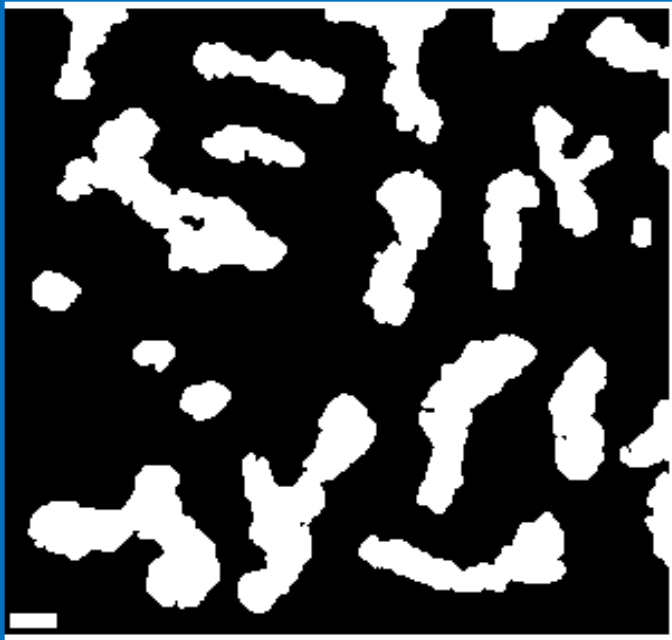
Exclusion of either AA or NO biosynthesis - AACOCF3 or L-NAME drugs



formation of immature networks, where several branches have partially formed, but have not been able to organize into a single structure

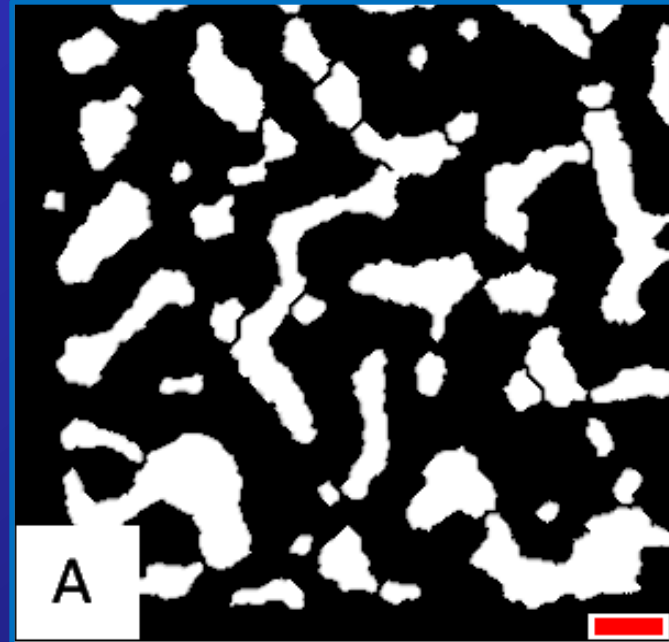
APPLICATIONS: TUMOR-DERIVED VASCULOGENESIS

Blocking cytoskeletal remodeling:
phalloidin-like compounds



formation of clumped, stunted, shorter
and thicker sprouts,

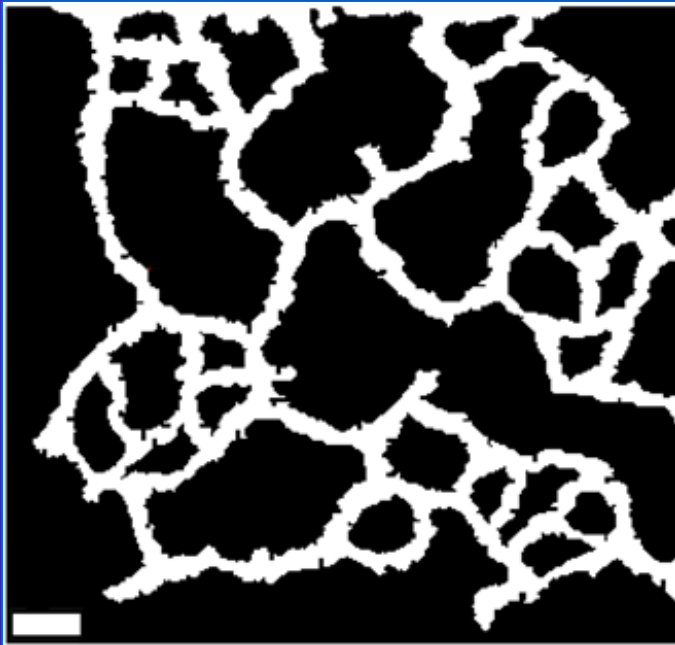
Disruption of cell persistent
movement



formation of immature and
swollen sprouts characterized
by large intervascular spaces

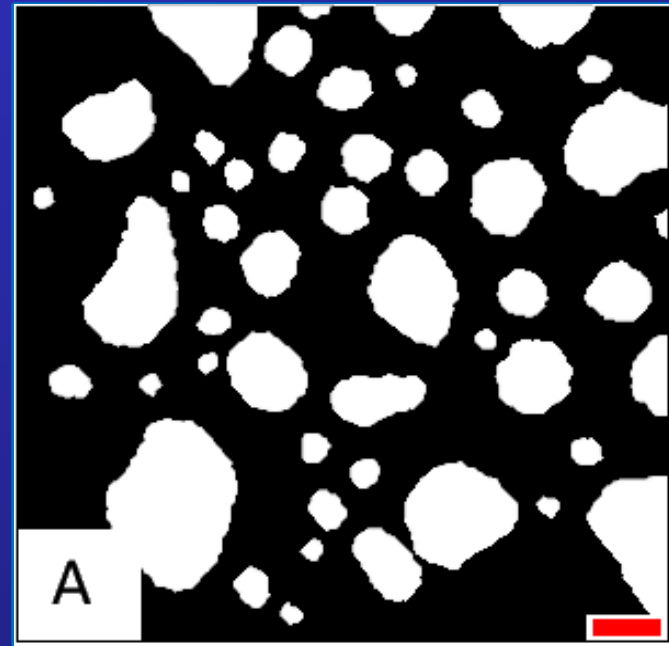
APPLICATIONS: TUMOR-DERIVED VASCULOGENESIS

Increasing VEGF degradation:



formation of a reduced-in-scale network

Disruption of chemotaxis



formation of poorly structured islands similar to those obtained by extinguish VEGF gradients



APPLICATIONS: TUMOR-DERIVED VASCULOGENESIS

The model allows to prove the efficacy some anti-angiogenic therapies that are currently in use or in trial and to test the potential of other biomedical intervention strategies

	EXISTING COMPOUND	P-VALUE (pct)	EFFICIENCY
VEGF UPTAKE	sorafenib, sunitinib, vatalanib	0.00082	+++
VEGF DEGRADATION		0.00234	++
CALCIUM ENTRY	CAI	0.00085	+++
AA PRODUCTION	AACOCF3	0.00425	+
NO PRODUCTION	L-NAME, L-NMMA	0.00473	+
CYTOSKELETAL REMODELING	phalloidin	0.00092	+++
PERSISTENCE		0.00139	++
CHEMOTAXIS		0.00097	+++
ADHESION	anti-VE-cadherin antibodies	0.00069	+++

TECs remain scattered

reduced-in-scale pattern

TECs remain scattered

formation of immature networks

clumped sprouts with large intervascular spaces

poorly structured islands

TECs remain scattered

BIBLIOGRAPHY



- ❖ Scianna, M., Merks, R. M. H., Preziosi, L., Medico, E., 2009. INDIVIDUAL CELL-BASED MODELS OF CELL SCATTER OF ARO AND MLP-29 CELLS IN RESPONSE TO HEPATOCYTE GROWTH FACTOR. *J TheorBiol*, 260 (1), 151 – 160.
- ❖ Giverso, C., Scianna, M., Preziosi, L., Lo Buono, N., Funaro, A., 2010. INDIVIDUAL CELL-BASED MODEL FOR IN-VITRO MESOTHELIAL INVASION OF OVARIAN CANCER. *Math Model Nat Phenom*, 5 (1), 203 – 223.
- ❖ Scianna, M., Munaron, L., Preziosi, L., 2011. A MULTISCALE HYBRID APPROACH FOR VASCULOGENESIS AND RELATED POTENTIAL BLOCKING THERAPIES. *Prog Biophys Mol Biol*, 106 (2), 450 – 462.
- ❖ Scianna, M., 2011. A MULTISCALE HYBRID MODEL FOR PRO-ANGIOGENIC CALCIUM SIGNALS IN A VASCULAR ENDOTHELIAL CELL. *Bull Math Biol*, 74 (6), 1253 - 1291.
- ❖ Lo Buono, N., Scianna, M., Bovino, P., Morone, S., Panotta, R., Ferrero, E., Giverso, C., Preziosi, L., Malavasi, F., Funaro, A., Ortolan, E., 2011. CD157 EXPRESSION ENHANCES INVASIVENESS OF OVARIAN CANCER CELLS AND INDUCES A MESENCHYMAL PHENOTYPE. *FEBS J*, 278, 218 – 219.
- ❖ Scianna, M., Munaron, L., 2011. MULTISCALE MODEL OF TUMOR-DERIVED CAPILLARY-LIKE NETWORK FORMATION. *NetwHeterog Media*, 6 (4), 597 – 624.

BIBLIOGRAPHY



- ❖ Scianna, M., Preziosi, L., 2012. A HYBRID CELLULAR POTTS MODEL DESCRIBING DIFFERENT MORPHOLOGIES OF TUMOR INVASION FRONTS. *Math Model Nat Phenom*, 7 (1), 78 - 104.
- ❖ Scianna, M., Preziosi, L., 2012. MULTISCALE DEVELOPMENTS OF THE CELLULAR POTTS MODEL. *Multiscale Model Simul*, 10 (2), 342-382.
- ❖ Munaron, L., Scianna, M., 2012. MULTISCALE COMPLEXITY OF CALCIUM SIGNALING: MODELING ANGIOGENESIS (review). *World J BiolChem*, 3(6), 121-126.
- ❖ Scianna, M., Preziosi, L., 2012. MODELLING THE INFLUENCE OF NUCLEUS ELASTICITY ON CELL INVASION IN FIBER NETWORKS AND MICROCHANNELS. *J Theor Biol*. In press.
- ❖ Scianna, M., 2012. MULTISCALE EXTENSIONS OF THE CELLULAR POTTS MODELS: TOWARD A NESTED-HYBRID APPROACH. *Communications in Applied and Industrial Mathematics*, 3 (1), e-411.
- ❖ Scianna, M., Preziosi, L., Wolf, K., 2013. A CELLULAR POTTS MODEL SIMULATING CELL MIGRATION ON AND IN MATRIX ENVIRONMENTS. *Math BiosciEng*, 10 (1), 235-261.
- ❖ Scianna, M., Preziosi, L., HYBRID CELLULAR POTTS MODEL FOR SOLID TUMOR GROWTH, in *New Challenges for Cancer Systems Biomedicine*, SIMAI Springer Series, d'Onofrio, P. Cerrai, and A. Gandolfieds., Springer-Verlag, 205– 224 (2012).